Supporting Information

Reaction of an N/Al FLP-Based Aluminum Hydride toward Alkyne: Deprotonated Alumination *versus* Hydroalumination with Regioselective *cis*-Addition Character

Yilin Chen, Wenjun Jiang, Bin Li, Gang Fu*, Shimin Chen, and Hongping Zhu*

State Key Laboratory of Physical Chemistry of Solid Surfaces, National Engineering Laboratory for Green Chemical Productions of Alcohols-Ethers-Esters, College of Chemistry and Chemical Engineering, Xiamen University, Xiamen, 361005, China

Content:

I. Crystal data and refinements

Table S1 Crystal data and refinements

	3	**7**
CCDC	1898700	1898701
Empirical formula	$C_{27}H_{28}AlNS_2$	$C_{44}H_{61}AlN_2Si_2$
formula weight	457.60	701.10
crystal system	Orthorhombic	Monoclinic
space group	*Pna*2(1)	*P*2(1)/*c*
a/Å	24.0988(9)	11.3883(5)
b/Å	8.7010(3)	19.6761(7)
c/Å	11.4918(5)	18.8444(7)
α/deg	90	90
β/deg	90	100.654(4)
γ/deg	90	90
V/Å^3	2409.64(16)	4149.8(3)
Z	4	4
ρ_{calcd}/g·cm^{-3}	1.261	1.122
μ/mm^{-1}	0.272	0.138
F(000)	968	1520
crystal size/mm^3	0.40×0.20×0.20	0.40×0.40×0.30
θ range/deg	2.45–27.00	2.34–24.00
index ranges	$-29 \le h \le 30$	$-6 \le h \le 13$
	$-11 \le k \le 5$	$-20 \le k \le 22$
	$-14 \le l \le 14$	$-21 \le l \le 20$
collected data	7072	14303
unique data	4642 (0.0285)	6484 (0.0491)
completeness to *θ*	99.8	99.7
data/restraints/parameters	4642/291/330	6484/0/461
GOF on F^2	1.036	1.046
final *R* indices [$I > 2$ (*I*)]	0.0457/0.1027	0.0609/0.1419
R indices (all data)	0.0548/0.1081	0.0802/0.1526
Largest diff peak/hole (e·Å^{-3})	0.214/–0.370	0.557/–0.361

[a] $R_1 = \sum(||F_o|-|F_c||)/\sum|F_o|$, $wR_2 = [\sum w(F_o^2-F_c^2)^2/\sum w(F_o^2)]^{1/2}$, GOF = $[\sum w(F_o^2-F_c^2)^2/(N_o-N_p)]^{1/2}$.

(to be continued)

	$\mathbf{8}_{0.5}\ C_6D_6$	**9**
CCDC	1898699	1898702
Empirical formula	$C_{41}H_{45}AlNP$	$C_{47}H_{58}AlNP_2Si_2$
formula weight	609.73	782.04
crystal system	Monoclinic	Monoclinic
space group	*P*2(1)/*c*	*P*2(1)/*c*
a/Å	13.9919(3)	11.3543(14)
b/Å	14.7539(4)	17.4839(10)
c/Å	18.7760(4)	22.6998(19)
α/deg	90	90
β/deg	92.469(2)	98.930(9)
γ/deg	90	90
V/Å^3	3872.43(16)	4451.7(7)
Z	4	4
ρ_{calcd}/g·cm^{-3}	1.046	1.167
μ/mm^{-1}	1.032	0.204
F(000)	1304	1672
crystal size/mm^3	0.30×0.30×0.20	0.28×0.26×0.20
θ range/deg	3.81–62.12	2.16–28.00
index ranges	$-16 \le h \le 15$	$-10 \le h \le 14$
	$-16 \le k \le 8$	$-18 \le k \le 23$
	$-21 \le l \le 14$	$-29 \le l \le 27$
collected data	12606	21386
unique data	6022 (0.0249)	10582 (0.0515)
completeness to *θ*	98.5	98.6
data/restraints/parameters	6022/0/387	10582/3/494
GOF on F^2	1.041	1.028
final *R* indices [$I > 2$ (*I*)]	0.0696/0.1986	0.0700/0.1296
R indices (all data)	0.0775/0.2129	0.1181/0.1461
Largest diff peak/hole (e·Å^{-3})	1.047/–0.259	0.659/–0.425

[a] $R_1 = \sum(||F_o|-|F_c||)/\sum|F_o|$, $wR_2 = [\sum w(F_o^2-F_c^2)^2/\sum w(F_o^2)]^{1/2}$, GOF = $[\sum w(F_o^2-F_c^2)^2/(N_o-N_p)]^{1/2}$.

Crystallographic data for compound [*o*-(TMP)H-C_6H_4]$AlCl_{0.28164}$(C≡$CPPh_2$)$_{2.71856}$

This is according to the reviewer's comment on the structure of compound **4**. We carefully recheck the previous structure solution and finally refined the structure into [*o*-(TMP)H-C_6H_4]$AlCl_{0.28164}$(C≡$CPPh_2$)$_{2.71856}$. In order to offer an approximate structure view to **4**, we showed crystallographic data of [*o*-(TMP)H-C_6H_4]$AlCl_{0.28164}$(C≡$CPPh_2$)$_{2.71856}$ herein along with the related bond parameters.

The crystallographic data of compound [*o*-(TMP)H-C_6H_4]$AlCl_{0.28164}$(C≡$CPPh_2$)$_{2.71856}$ (previously named as **4**) was collected on a Rigaku Oxford Diffraction system. During measurements a graphite-monochromatic Cu-K_α radiation (λ = 1.54178 Å) was applied. Absorption corrections were all employed using the spherical harmonics program (multi-scan type). The structure was solved by direct methods (SHELXS-96)[15] and refined against F^2 using SHELXL-2014.[16] In

general, the non-hydrogen atoms were located by difference Fourier synthesis and refined anisotropically, and hydrogen atoms were included using a riding mode with U_{iso} tied to the U_{iso} of the parent atoms unless otherwise specified. In [*o*-(TMP)H-C_6H_4]$AlCl_{0.28164}(C{\equiv}CPPh_2)_{2.71856}$, the Cl atoms and $C{\equiv}CPPh_2$ groups were disordered, which were treated by the PART method. Final refinement gave Cl(1) (0.12443) and C(3)C(4)P(2)C(34)C(35)C(36)C(37)C(38)C(39)C(40)C(41)C(42)C(43)C(44)C(45) (0.87557) and Cl(2) (0.15837) and C(5)C(6)P(3)C(46)C(47)C(48)C(49)C(50)C(51)C(52)C(53)C(54)-C(55)C(56)C(57) (0.84163). A summary of cell parameters, data collection, and structure solution and refinements is given in Table S2 and the crystal structure is shown in Figure S11.

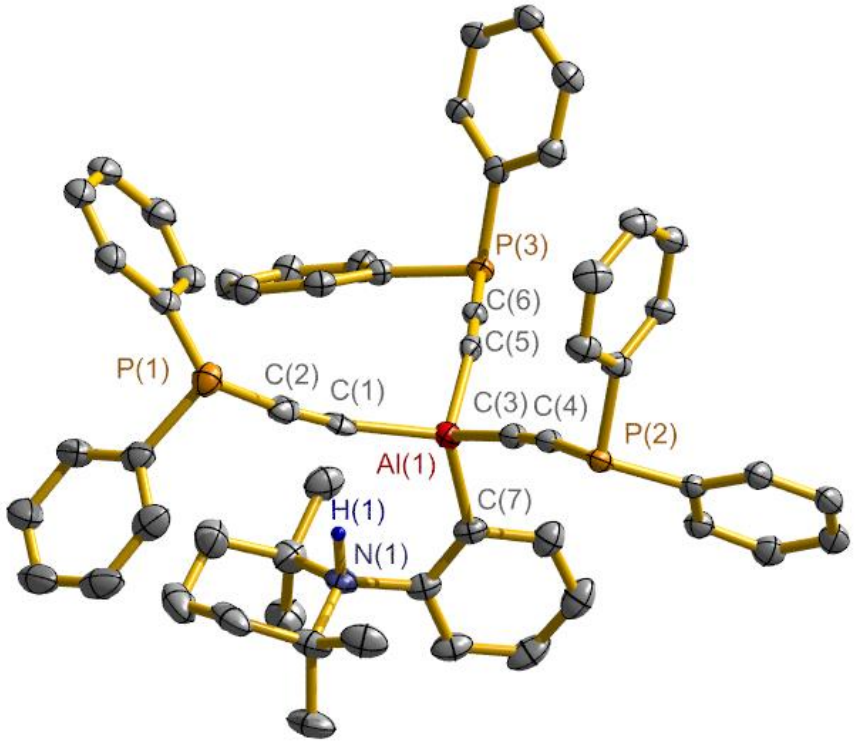

Figure S11. X-ray crystal structure of [*o*-(TMP)H-C_6H_4]$AlCl_{0.28164}(C{\equiv}CPPh_2)_{2.71856}$ with thermal ellipsoids at 50% probability level. The NH hydrogen atom is enhanced and the other H atoms and the Cl atoms are omitted for clarity. Selected bond lengths (Å) and angles (°): Al(1)–C(1) 2.023(3), Al(1)–C(3) 1.984(5), Al(1)–C(5) 2.051(7), Al(1)–C(7) 2.006(3), C(1)–C(2) 1.146(4), C(3)–C(4) 1.160(6), C(5)–C(6) 1.132(8), Al(1)–Cl(1) 2.405(10), Al(1)–Cl(2) 2.318(8); C(1)–Al(1)–C(3) 107.79(15), C(1)–Al(1)–C(5) 108.0(2), C(3)–Al(1)–C(5) 114.1(3), C(1)–Al(1)–C(7) 115.13(11), C(3)–Al(1)–C(7) 106.81(16), C(5)–Al(1)–C(7) 105.2(3).

Crystallographic data for compound (*o*-TMP-C_6H_4)AlH(CPh=CHEt) (6)

This is according to the reviewer's comment. We repeated the reaction of **1** and PhC≡CEt and obtained the single-crystals. The solution data was not good probably due to not good quality of the crystals. In order to offer an approximate structure view to **6**, we showed crystallographic data herein along with the related bond parameters.

The crystallographic data of compound **6** was collected on a Rigaku Oxford Diffraction system. During measurements a graphite-monochromatic Cu-K_α radiation (λ = 1.54178 Å) was applied. Absorption corrections were all employed using the spherical harmonics program (multi-scan type). The structure was solved by direct methods (SHELXS-96)[15] and refined against F^2 using SHELXL-2014.[16] In general, the non-hydrogen atoms were located by difference Fourier synthesis and refined anisotropically, and hydrogen atoms were included using a riding mode with U_{iso} tied to the U_{iso} of the parent atoms unless otherwise specified. In **6**, a half moiety was disclosed and the whole molecule as a dimer was obtained by the centrosymmetric operation. The H atom attached at Al atom was located from the difference Fourier synthesis and refined isotropically. A summary of cell parameters, data collection, and structure solution and refinements is given in Table S2 and the crystal structure is shown in Figure S12.

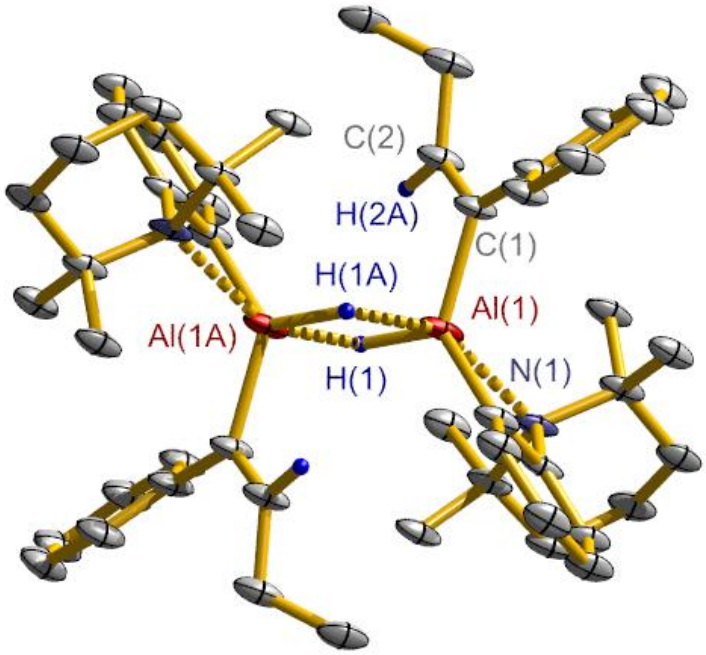

Figure S12. X-ray crystal structure of **6** with thermal ellipsoids at 50% probability level. The =CH and AlH hydrogen atoms are enhanced and the other H atoms are omitted for clarity. Selected bond lengths (Å) and angles (°): Al(1)–C(1) 1.984(4), Al(1)–C(11) 1.958(4), Al(1)–N(1) 2.429(4), Al(1)–H(1) 1.47(5), Al(1)–H(1A) 1.847(5), C(1)–C(2) 1.329(9); C(1)–Al(1)–C(11) 127.87(18), C(1)–Al(1)–N(1) 112.72(18), N(1)–Al(1)–C(11) 64.48(17). Symmetric code: –x, –y, –z+1.

Table S2 Crystal data and refinements

	4	**6**$_2$
Empirical formula	$C_{53.31}H_{50.18}AlCl_{0.28}NP_{2.72}$	$C_{50}H_{68}Al_2N_2$
formula weight	825.97	751.02
crystal system	Monoclinic	Monoclinic
space group	*P*2(1)/*c*	*P*2(1)/*n*
a/Å	8.93330(10)	9.3269(2)
b/Å	22.33240(10)	19.3988(5)
c/Å	23.8932(2)	12.1298(2)
α/deg	90	90
β/deg	92.5560(10)	90.591(2)
γ/deg	90	90
V/Å^3	4762.00(7)	2191.54(8)
Z	4	2
ρ_{calcd}/g·cm^{-3}	1.152	1.137
μ/mm^{-1}	1.640	0.850
F(000)	1742	816
crystal size/mm^3	0.30×0.30×0.20	0.20×0.20×0.10
θ range/deg	3.96–74.09	4.30–72.47
index ranges	$-11 \le h \le 10$	$-11 \le h \le 10$
	$-27 \le k \le 27$	$-23 \le k \le 21$
	$-29 \le l \le 28$	$-15 \le l \le 14$
collected data	61274	16863
unique data	9486 (0.0455)	4308 (0.1555)
completeness to θ	98.1	99.0
data/restraints/parameters	9486/1512/587	4308/0/254
GOF on F^2	1.042	2.111
final *R* indices [$I > 2$ (*I*)]	0.0754/0.2095	0.1528/0.4372
R indices (all data)	0.0774/0.2119	0.1695/0.4806
Largest diff peak/hole (e·Å^{-3})	1.026/–0.778	0.852/–2.151

[a] $R_1 = \sum(||F_o|-|F_c||)/\sum|F_o|$, $wR_2 = [\sum w(F_o^2-F_c^2)^2/\sum w(F_o^2)]^{1/2}$, GOF = $[\sum w(F_o^2-F_c^2)^2/(N_o-N_p)]^{1/2}$.

II. Collected ^{1}H, ^{13}C and/or ^{29}Si and ^{31}P spectra of compounds 2-10 and [*o*-(TMP)H-C$_6$H$_4$]Al(C≡CPh)$_2$(C≡CPPh$_2$).

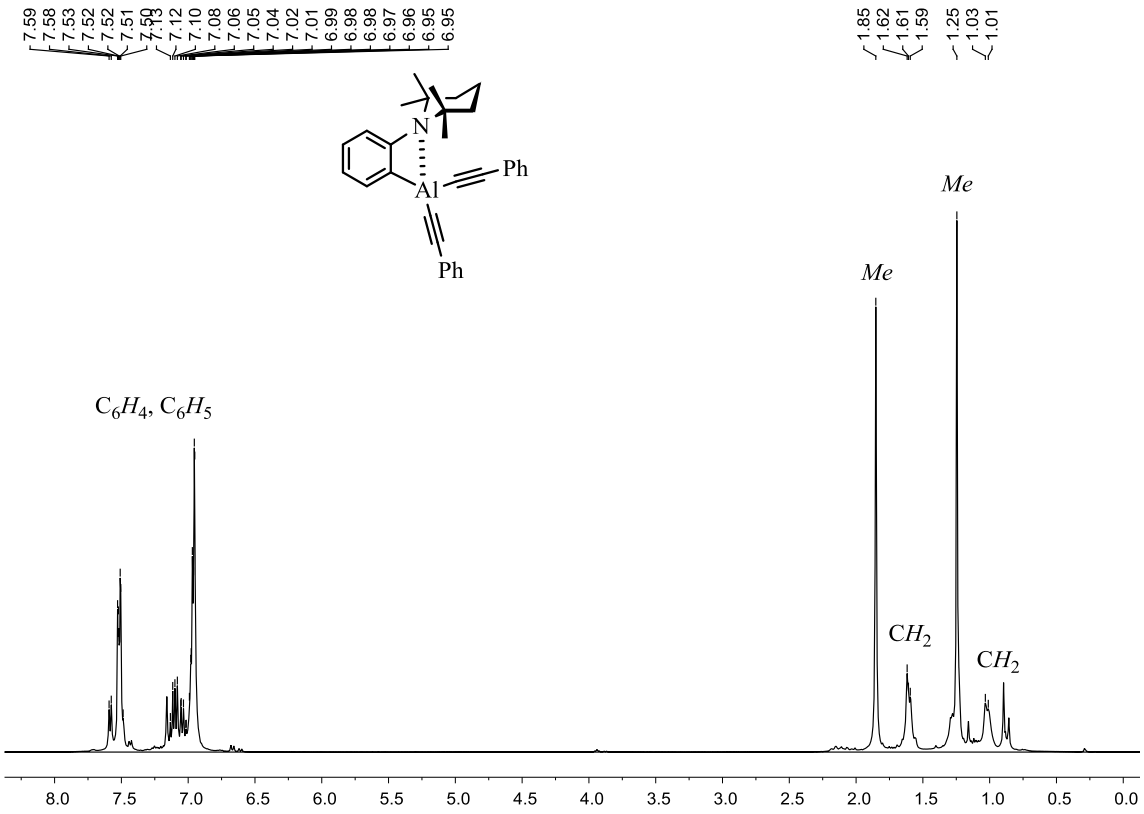

Figure S1-1. ^{1}H NMR spectrum of **2** in C_6D_6 at 298 K

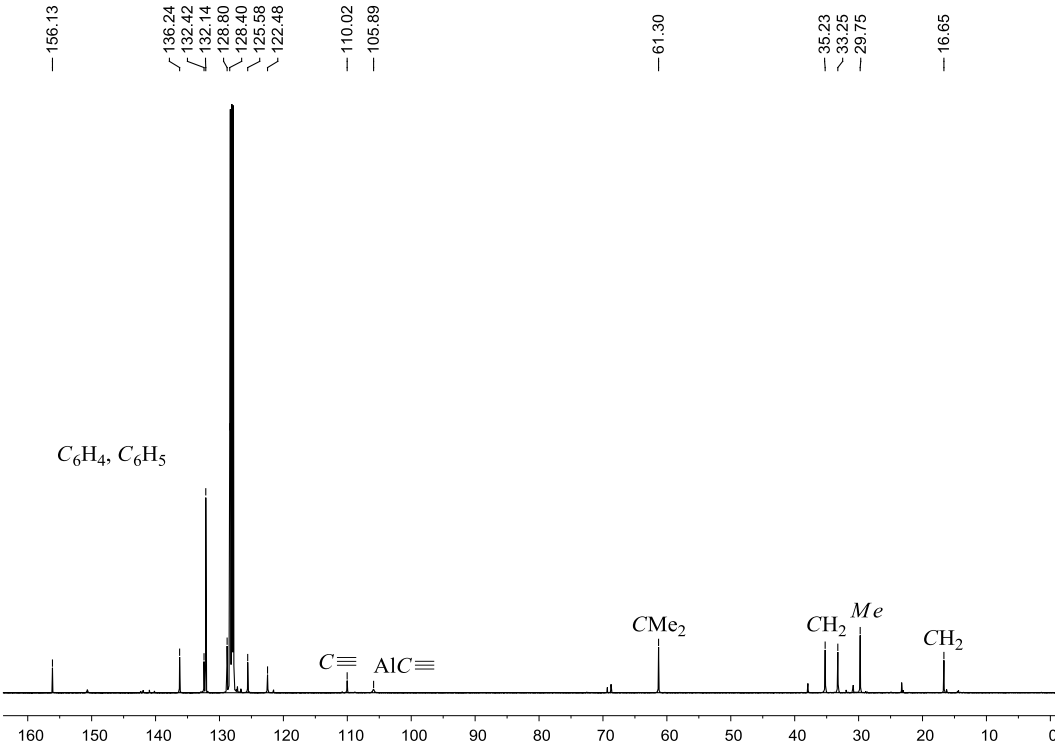

Figure S1-2. ^{13}C NMR spectrum of **2** in C_6D_6 at 298 K

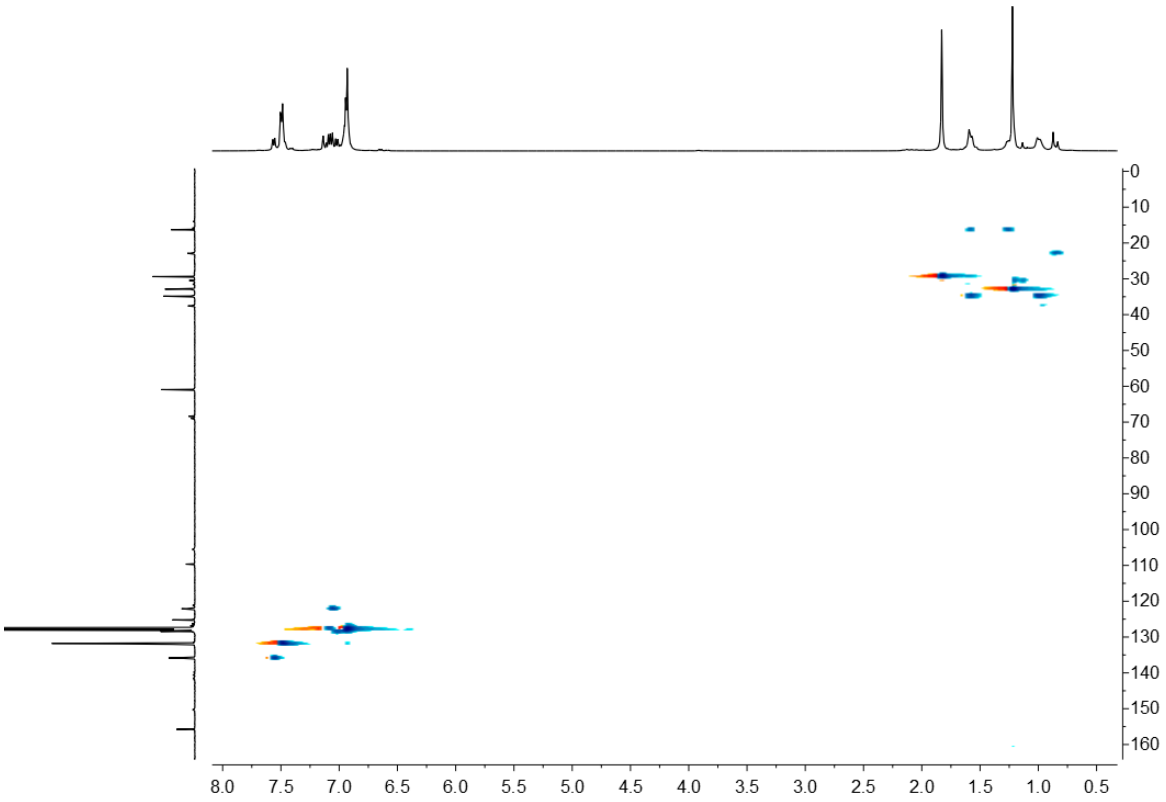

Figure S1-3. $^{1}H,^{13}C$-HSQC spectrum of **2** in C_6D_6 at 298 K

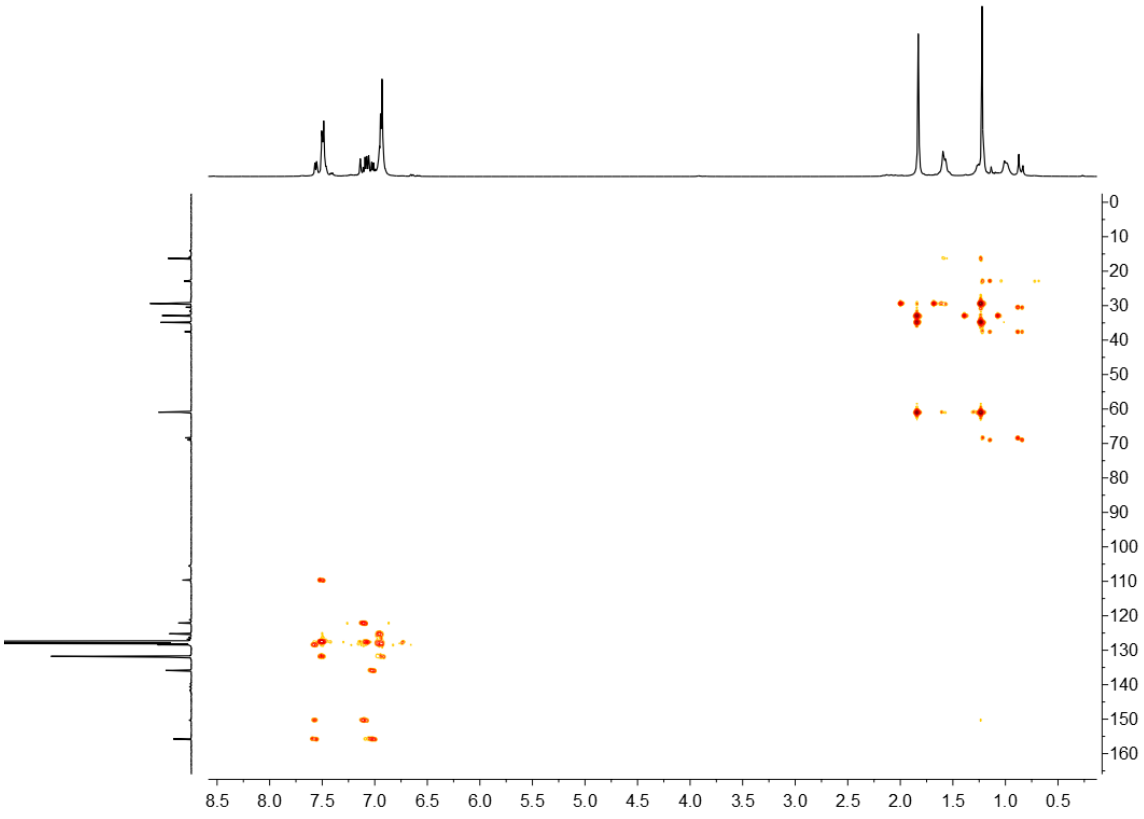

Figure S1-4. $^{1}H,^{13}C$-HMBC spectrum of **2** in C_6D_6 at 298 K

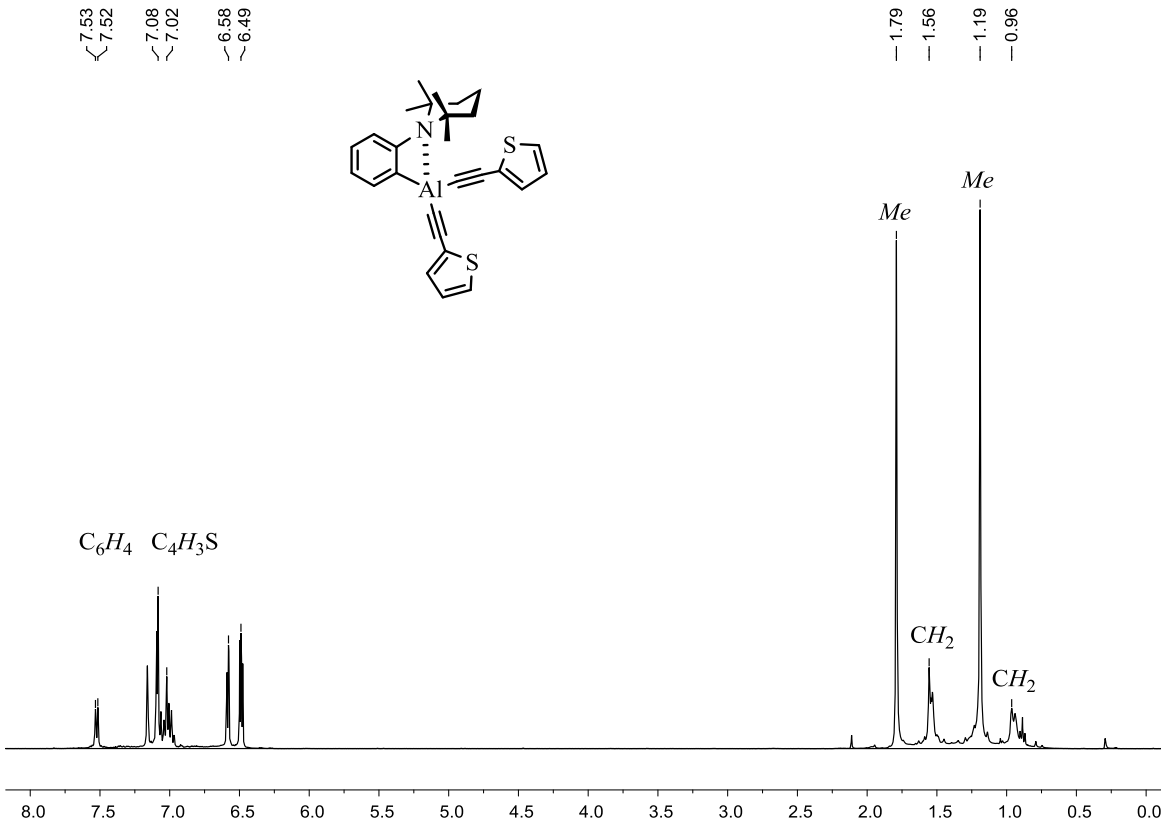

Figure S2-1. ^{1}H NMR spectrum of **3** in C_6D_6 at 298 K

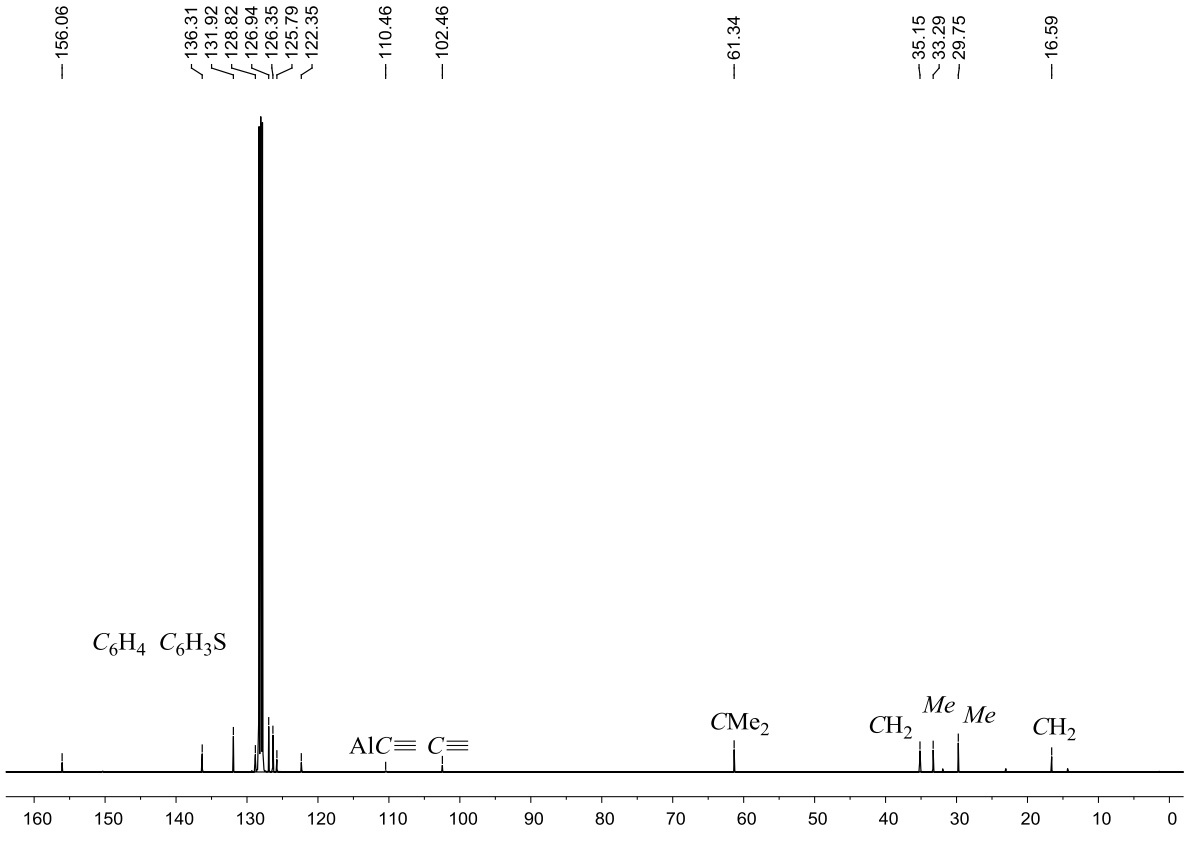

Figure S2-2. ^{13}C NMR spectrum of **3** in C_6D_6 at 298 K

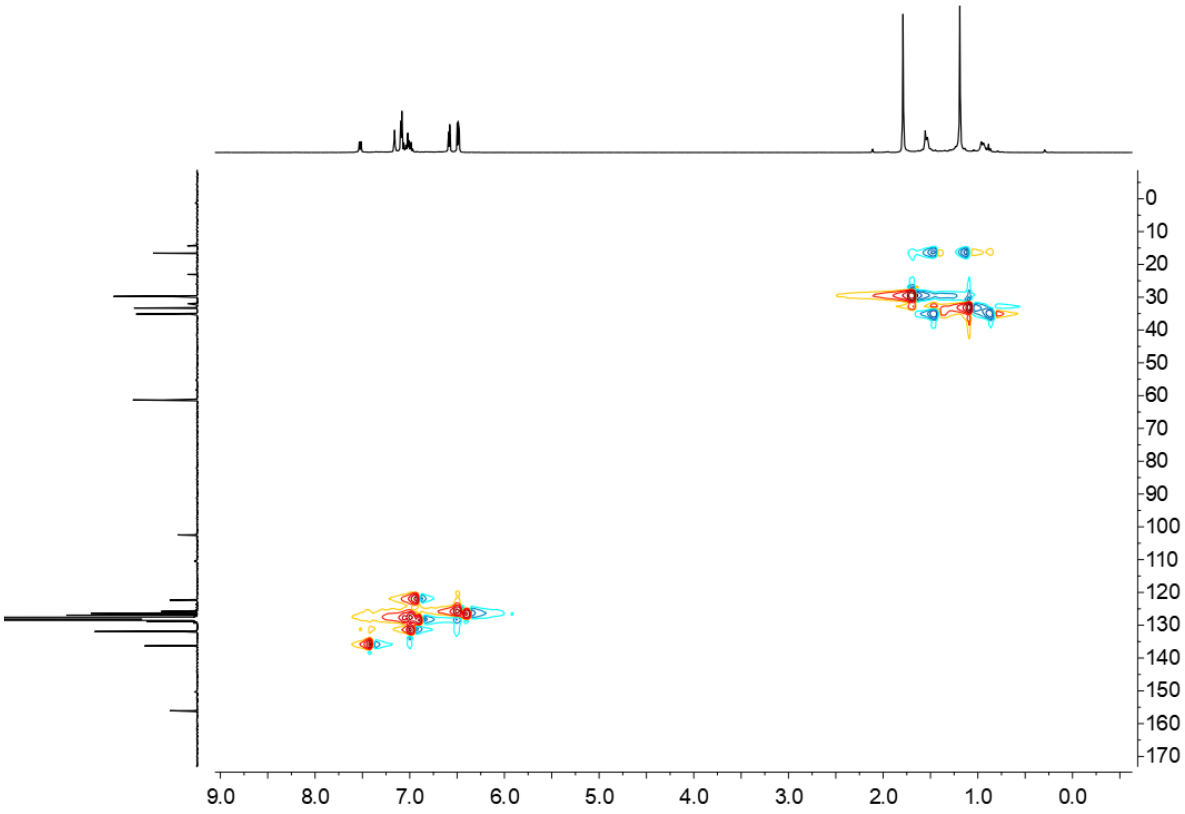

Figure S2-3. $^{1}H,^{13}C$-HSQC spectrum of **3** in C_6D_6 at 298 K

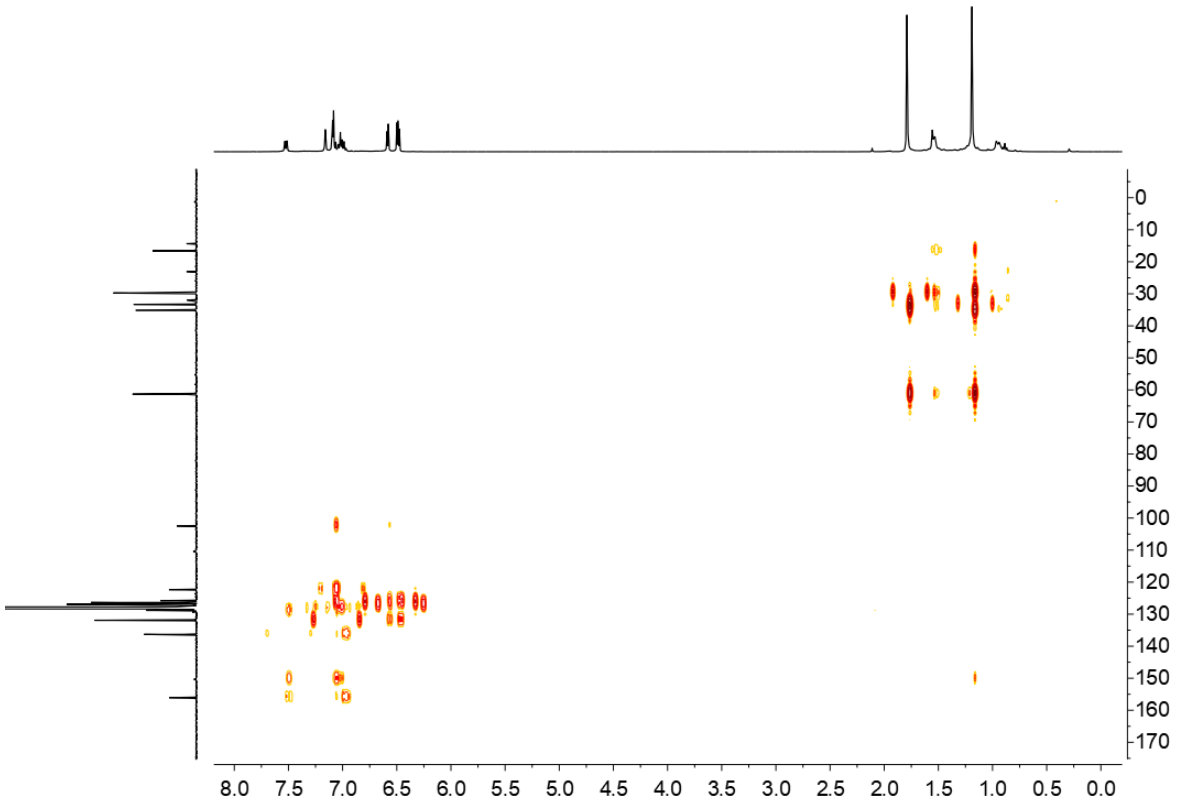

Figure S2-4. $^{1}H,^{13}C$-HMBC spectrum of **3** in C_6D_6 at 298 K

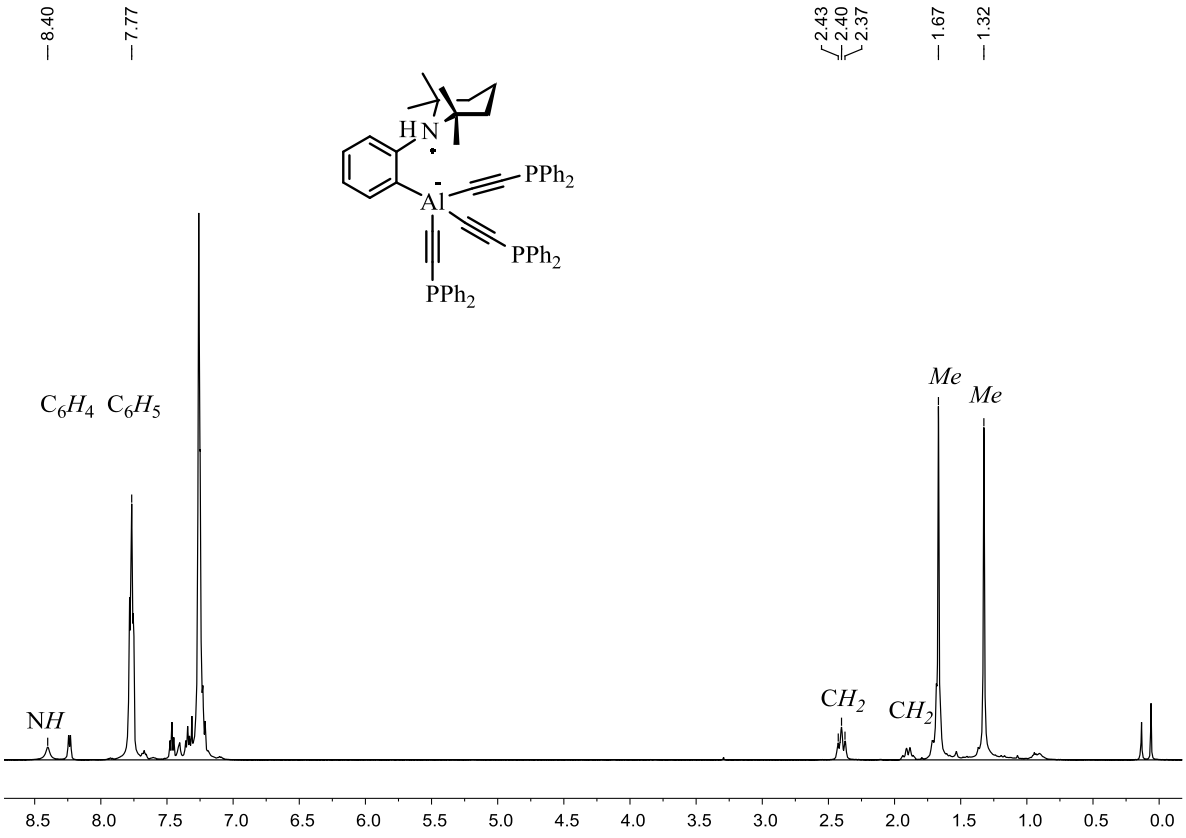

Figure S3-1. ^{1}H NMR spectrum of **4** in $CDCl_3$ at 298 K

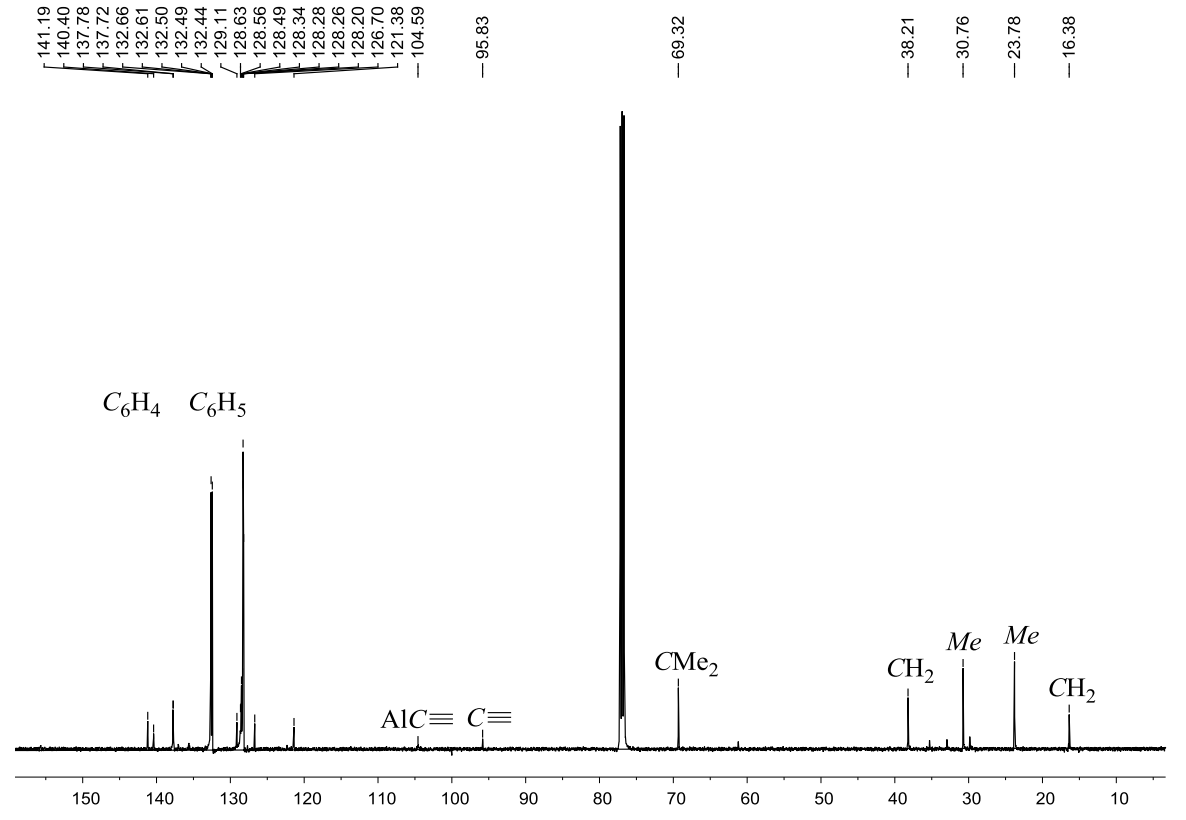

Figure S3-2. ^{13}C NMR spectrum of **4** in $CDCl_3$ at 298 K

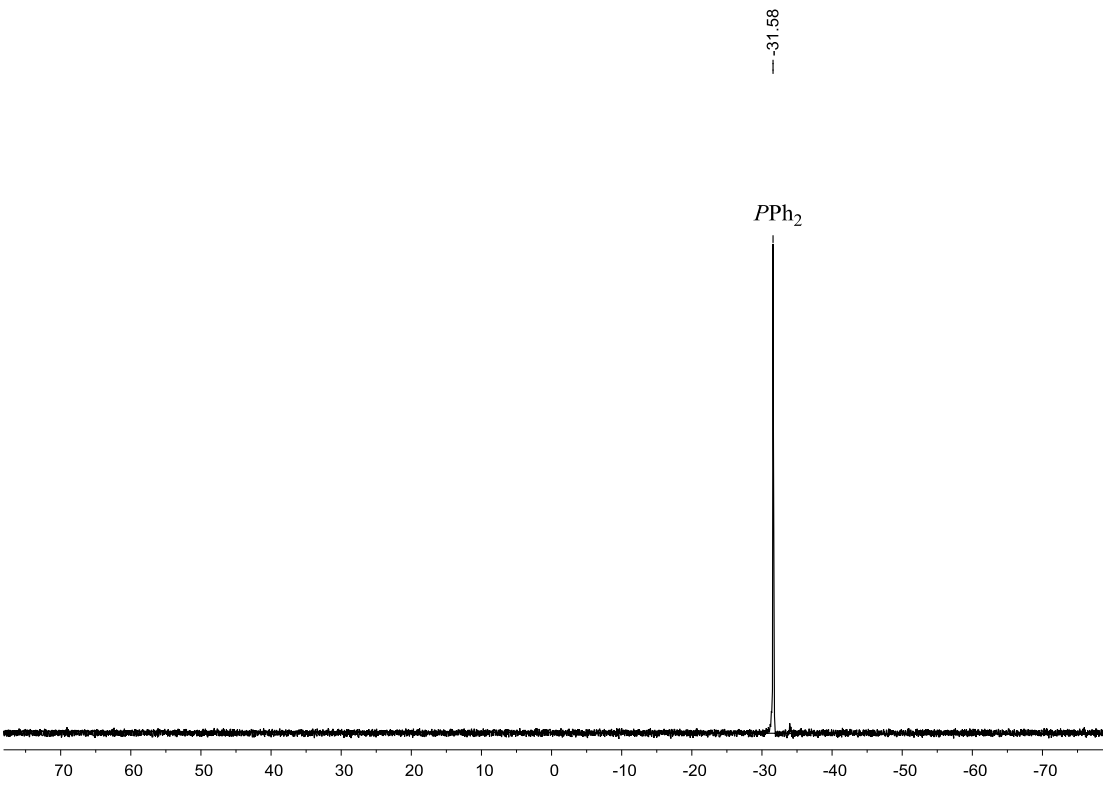

Figure S3-3. ^{31}P NMR spectrum of **4** in $CDCl_3$ at 298 K

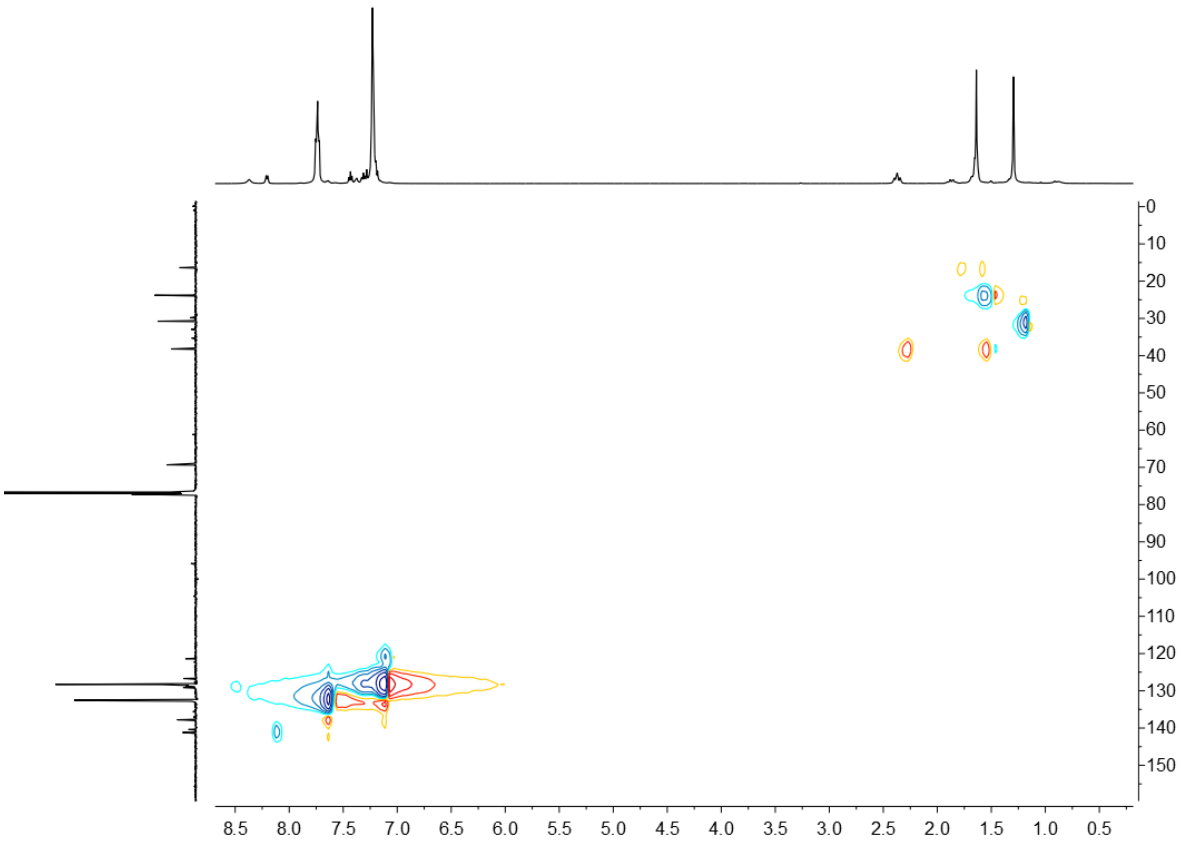

Figure S3-4. ^{1}H,^{13}C-HSQC spectrum of **4** in $CDCl_3$ at 298 K

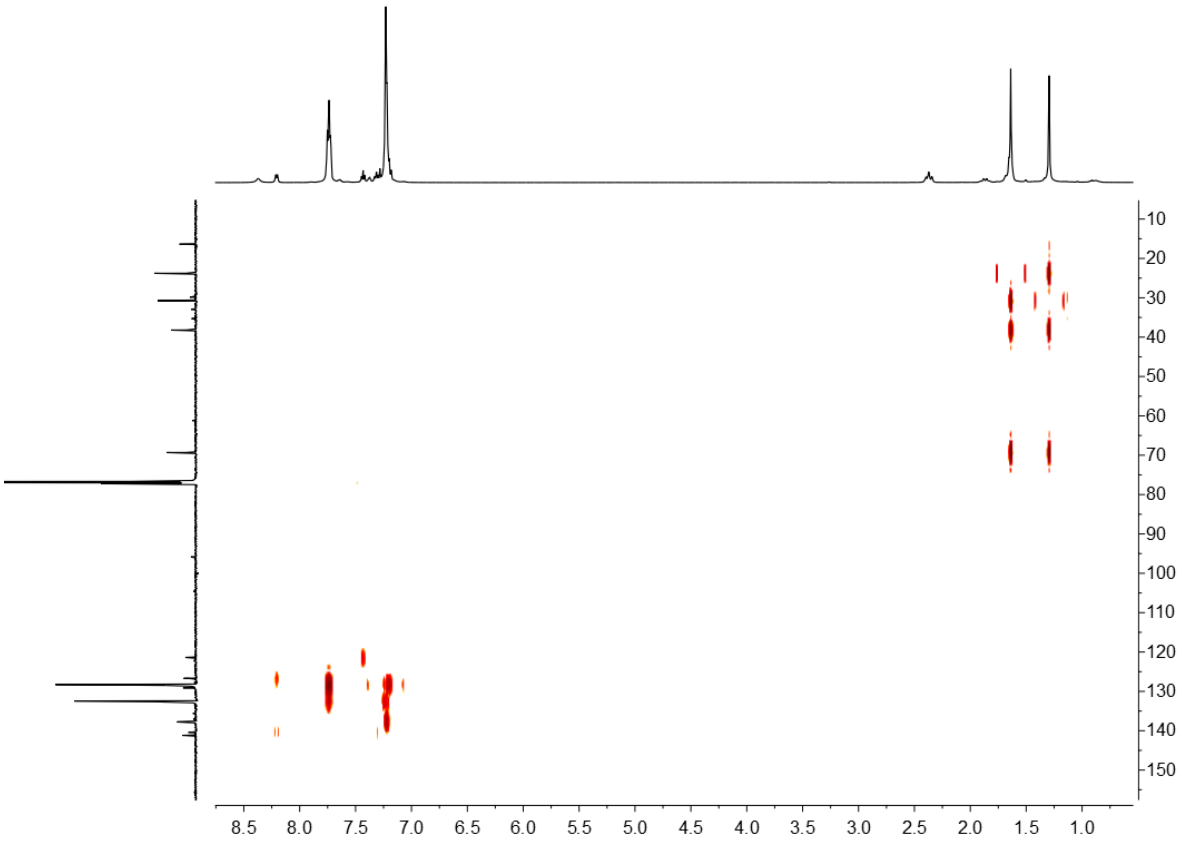

Figure S3-5. $^{1}H,^{13}C$-HMBC spectrum of **4** in $CDCl_3$ at 298 K

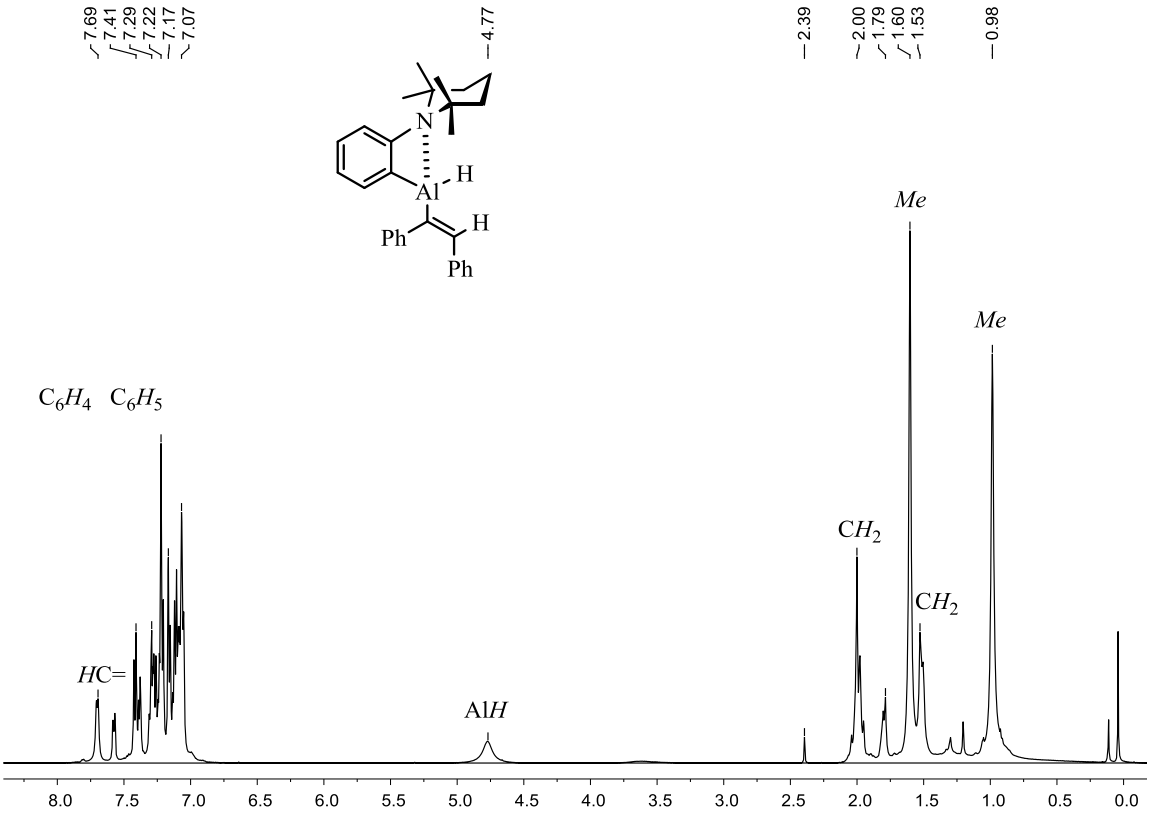

Figure S4-1. ^{1}H NMR spectrum of **5** in $CDCl_3$ at 298 K

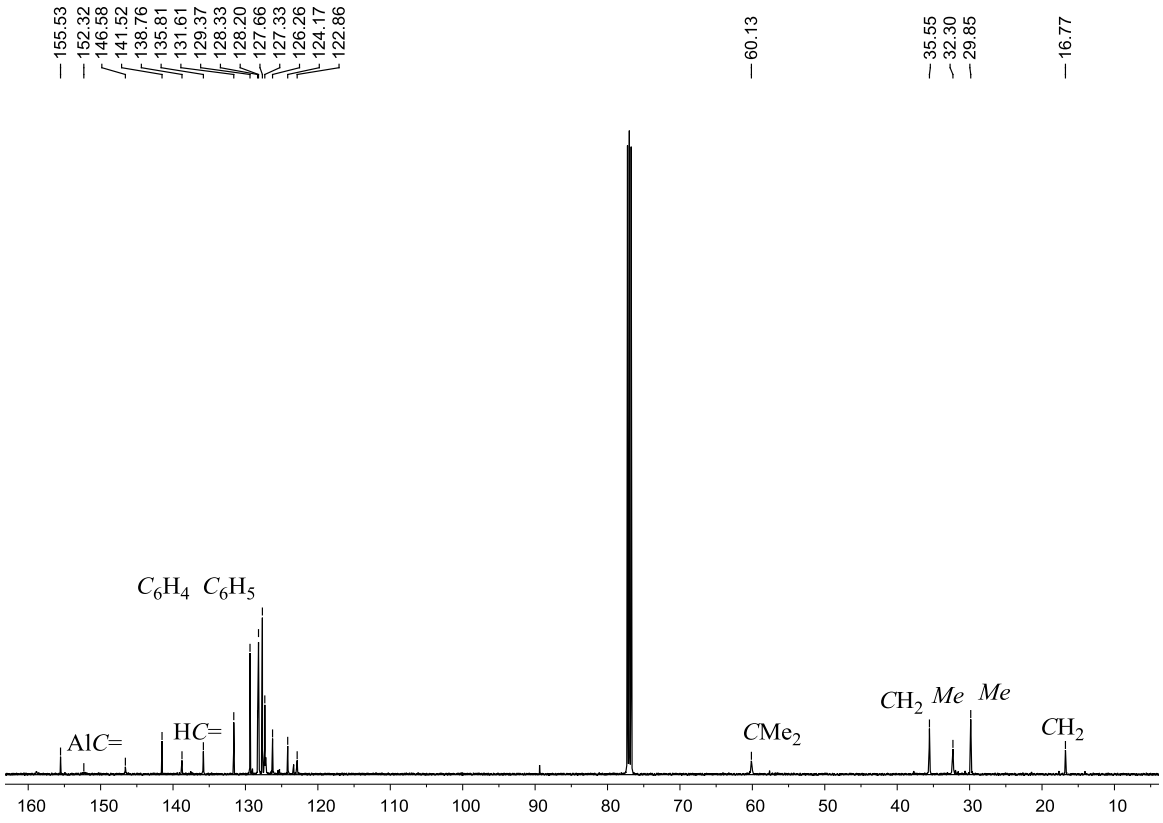

Figure S4-2. ^{13}C NMR spectrum of **5** in $CDCl_3$ at 298 K

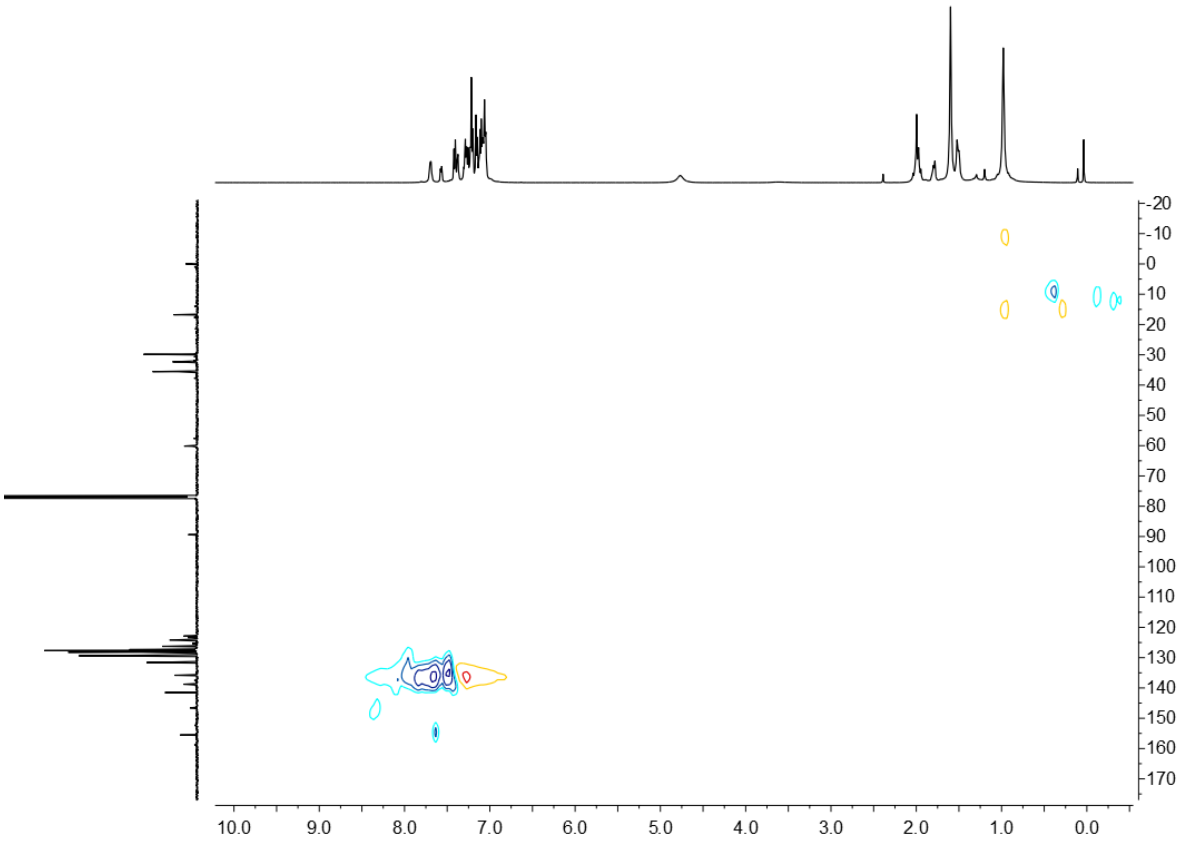

Figure S4-3. ^{1}H,^{13}C-HSQC spectrum of **5** in $CDCl_3$ at 298 K

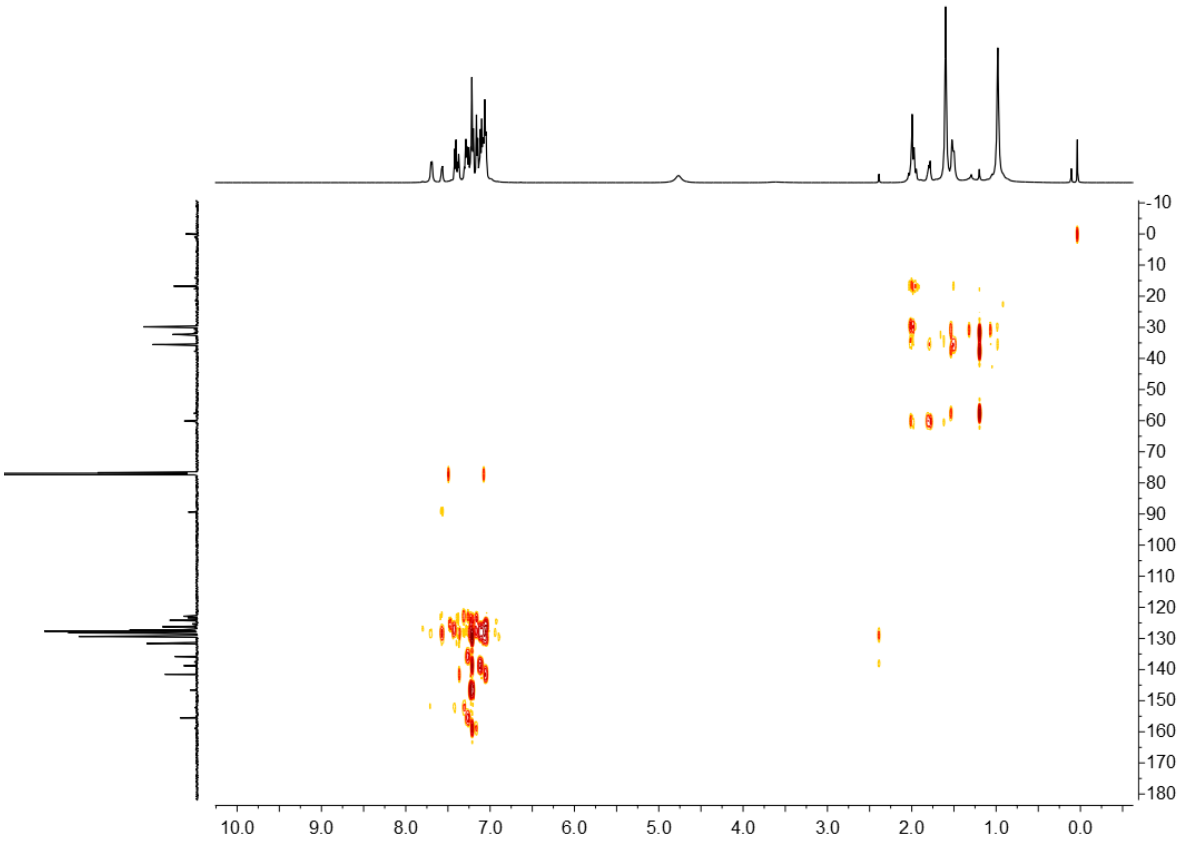

Figure S4-4. $^{1}H,^{13}C$-HMBC spectrum of **5** in $CDCl_3$ at 298 K

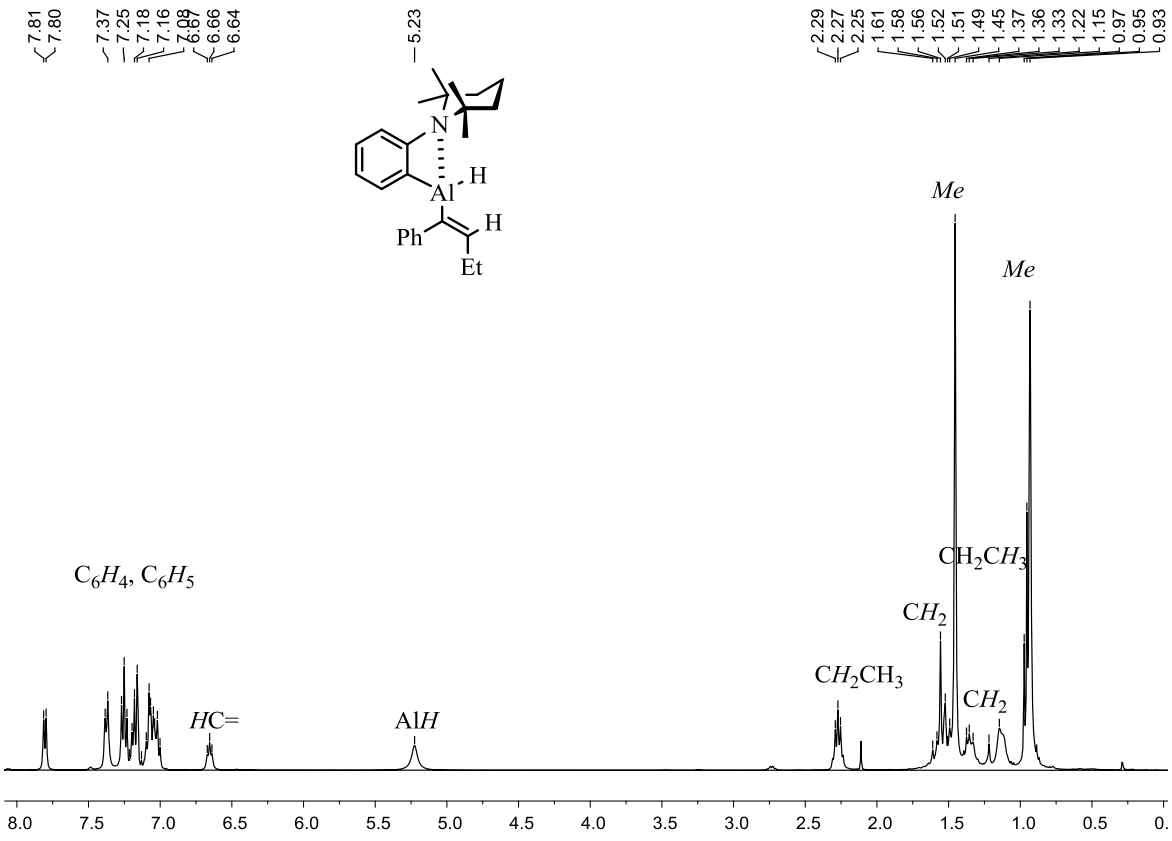

Figure S5-1. ^{1}H NMR spectrum of **6** in C_6D_6 at 298 K

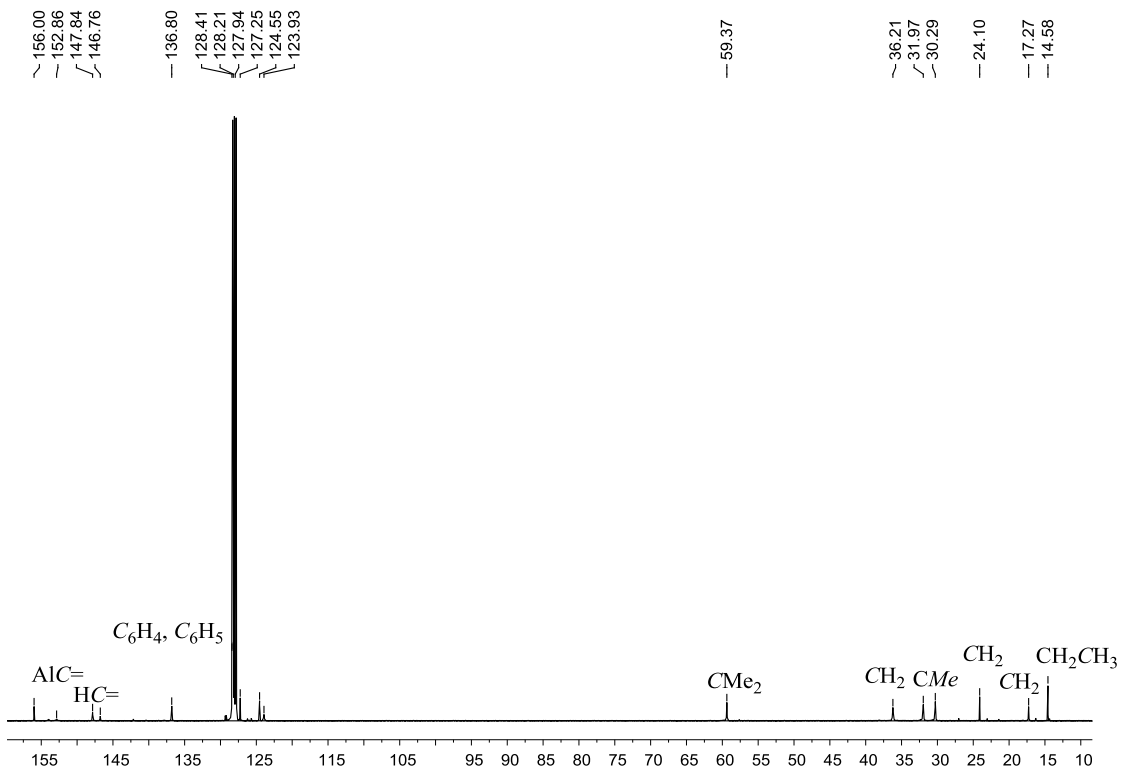

Figure S5-2. ^{13}C NMR spectrum of **6** in C_6D_6 at 298 K

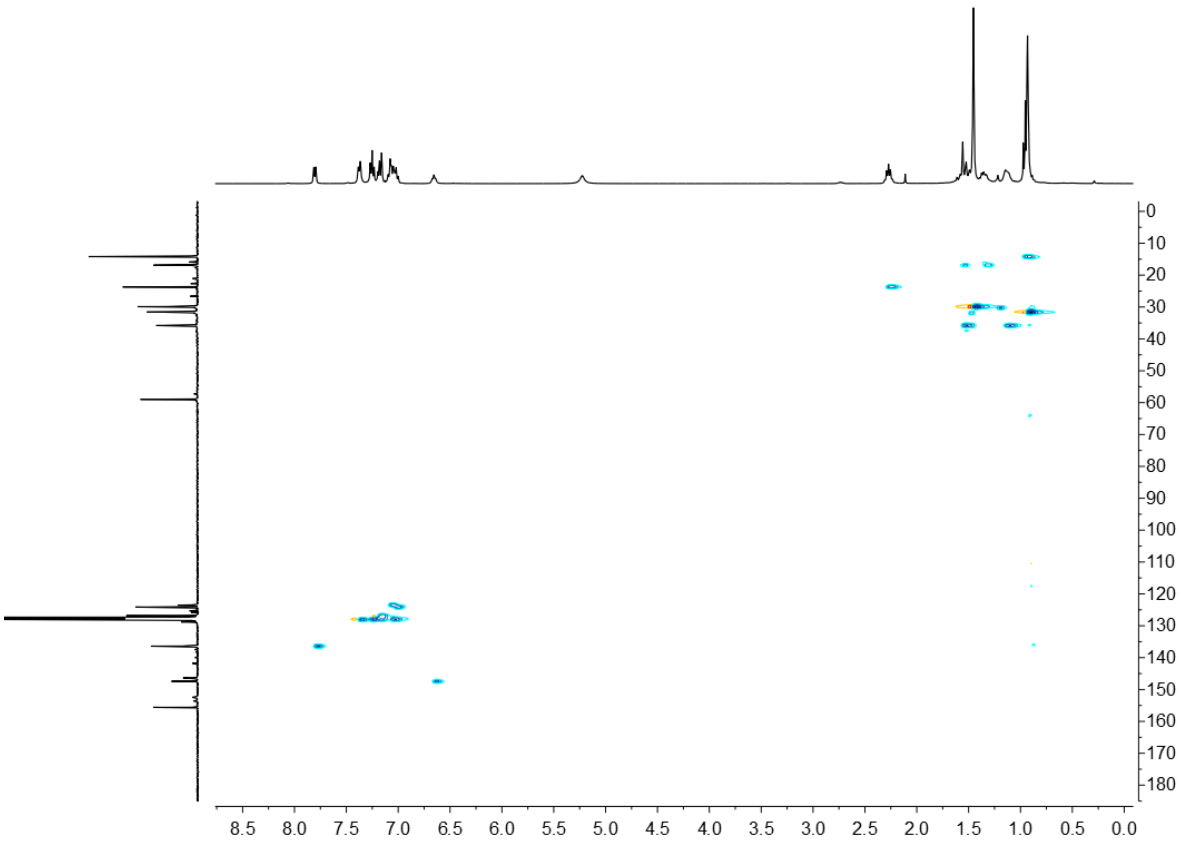

Figure S5-3. $^{1}H,^{13}C$-HSQC spectrum of **6** in C_6D_6 at 298 K

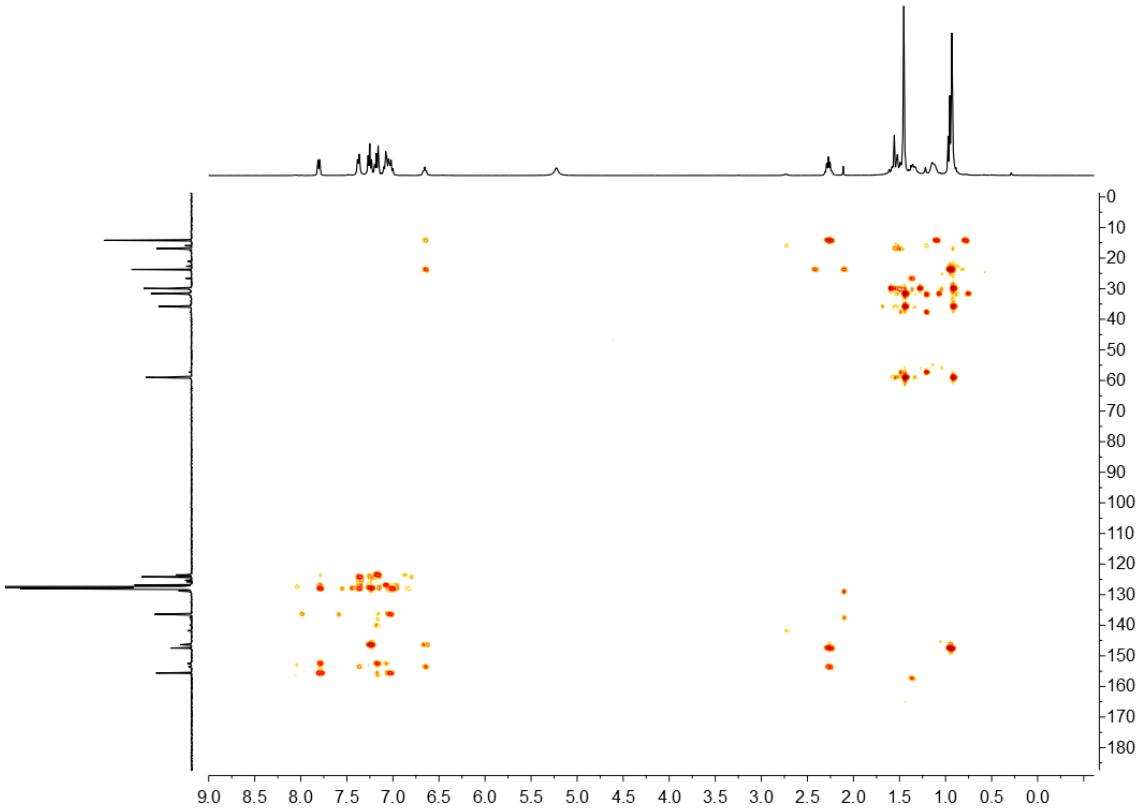

Figure S5-4. $^{1}H,^{13}C$-HMBC spectrum of **6** in C_6D_6 at 298 K

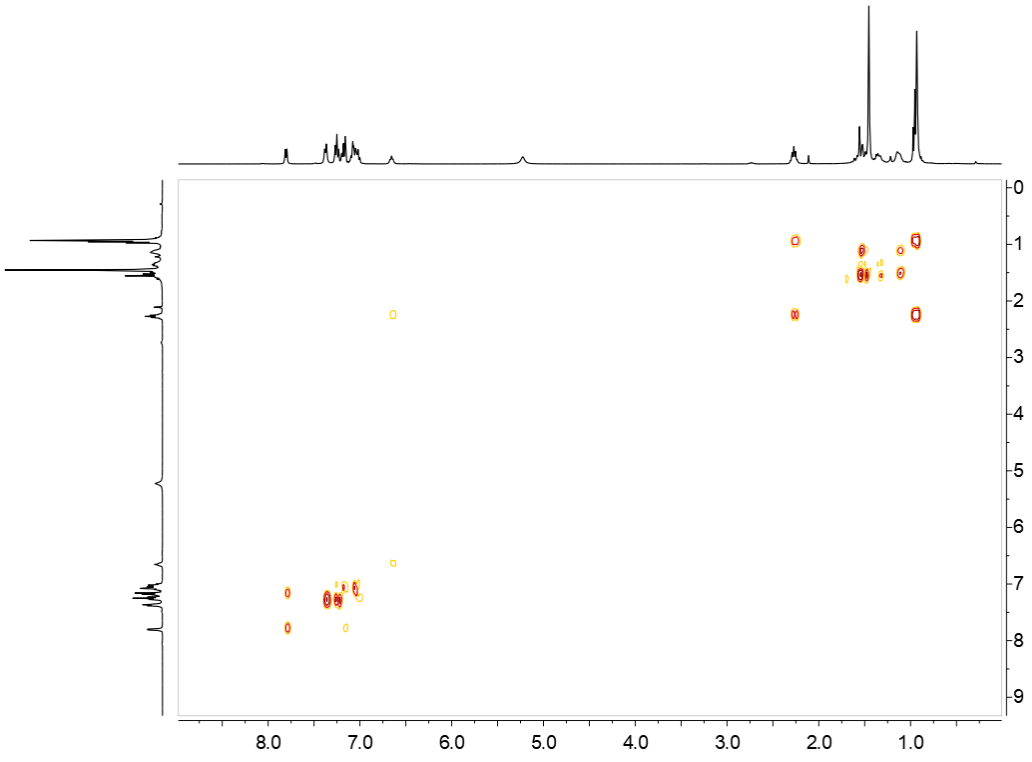

Figure S5-5. $^{1}H,^{1}H$-COSY spectrum of **6** in C_6D_6 at 298 K

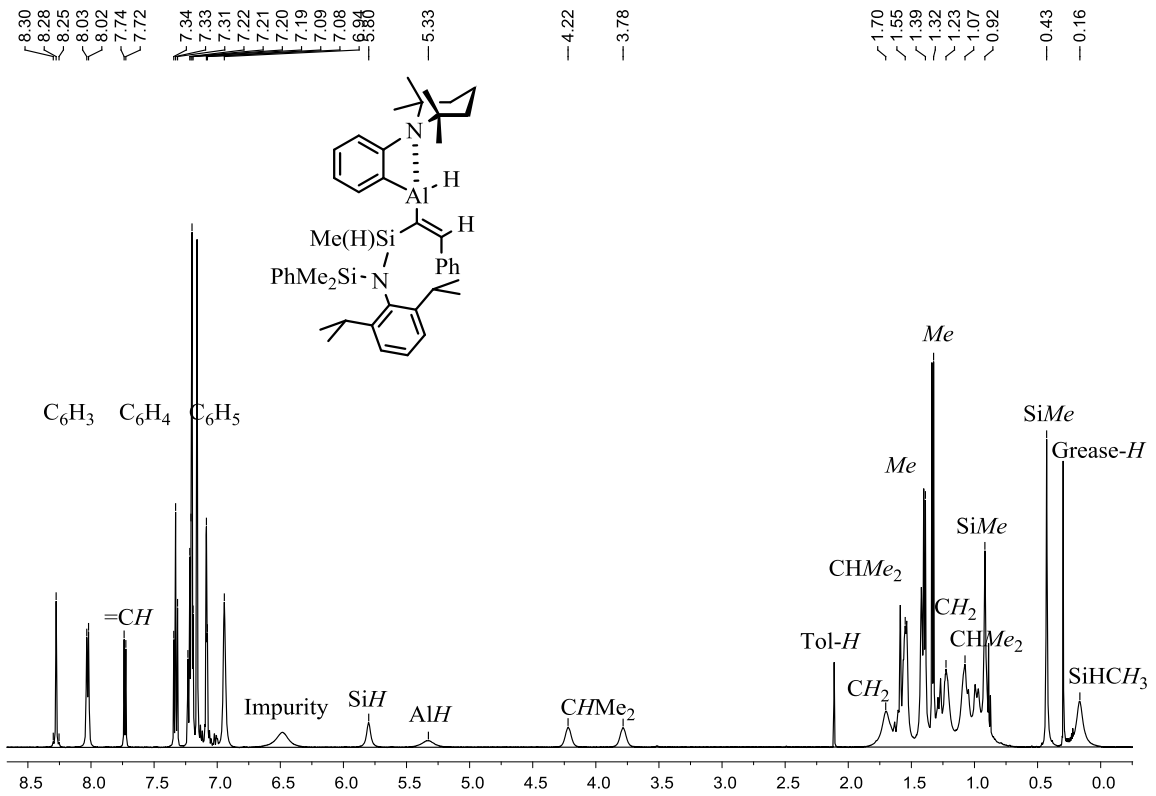

Figure S6-1. ^{1}H NMR spectrum of **7** in C_6D_6 at 298 K

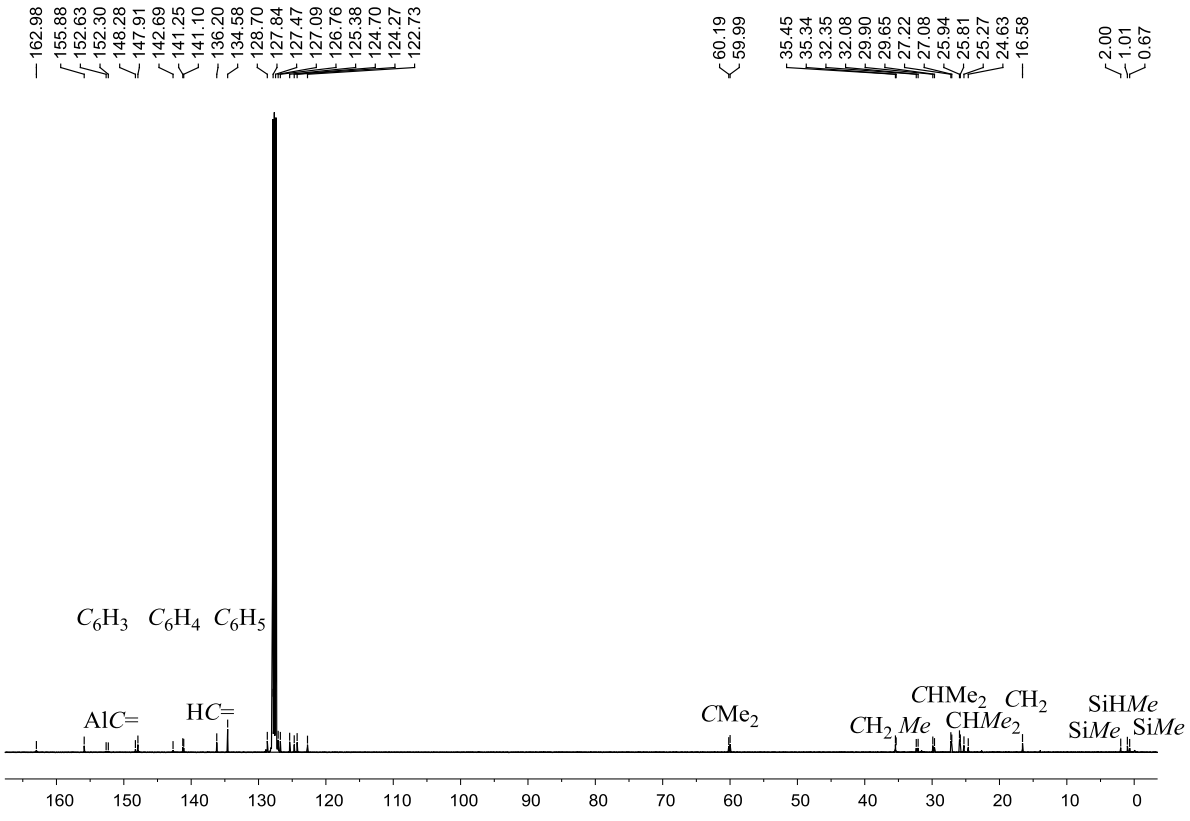

Figure S6-2. ^{13}C NMR spectrum of **7** in C_6D_6 at 298 K

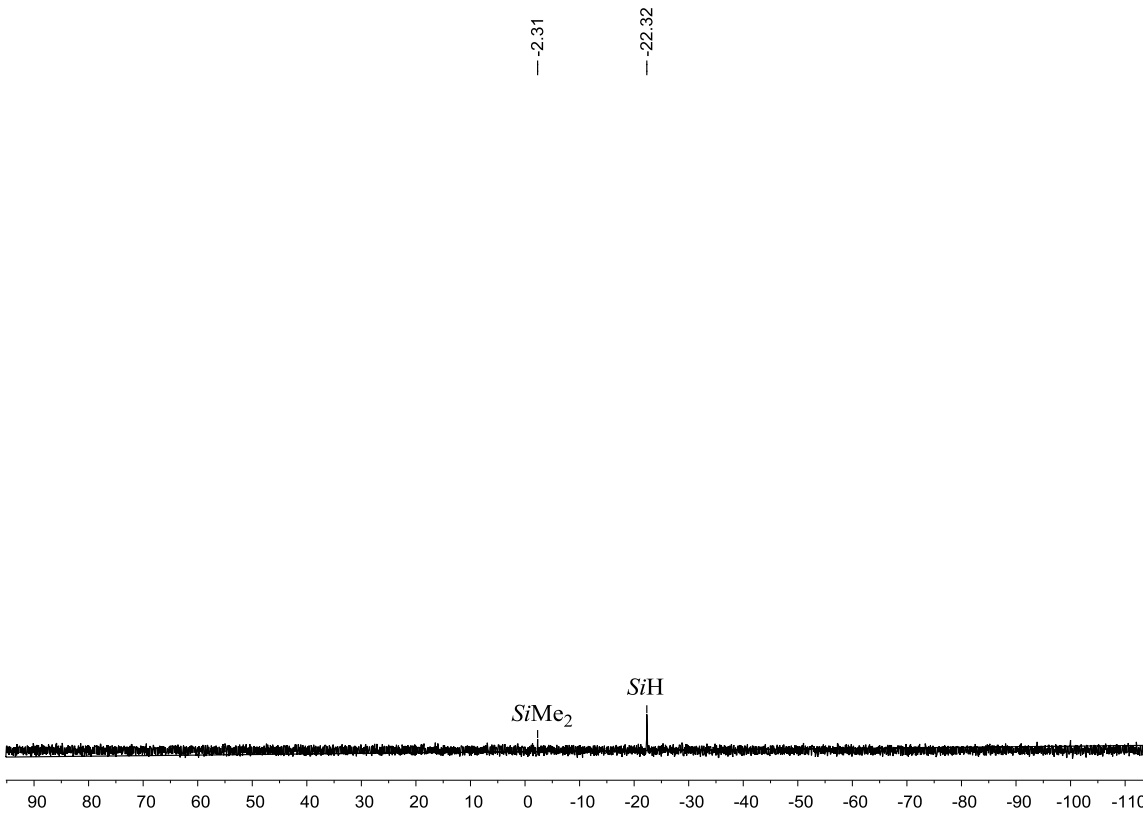

Figure S6-3. ^{29}Si NMR spectrum of **7** in C_6D_6 at 298 K

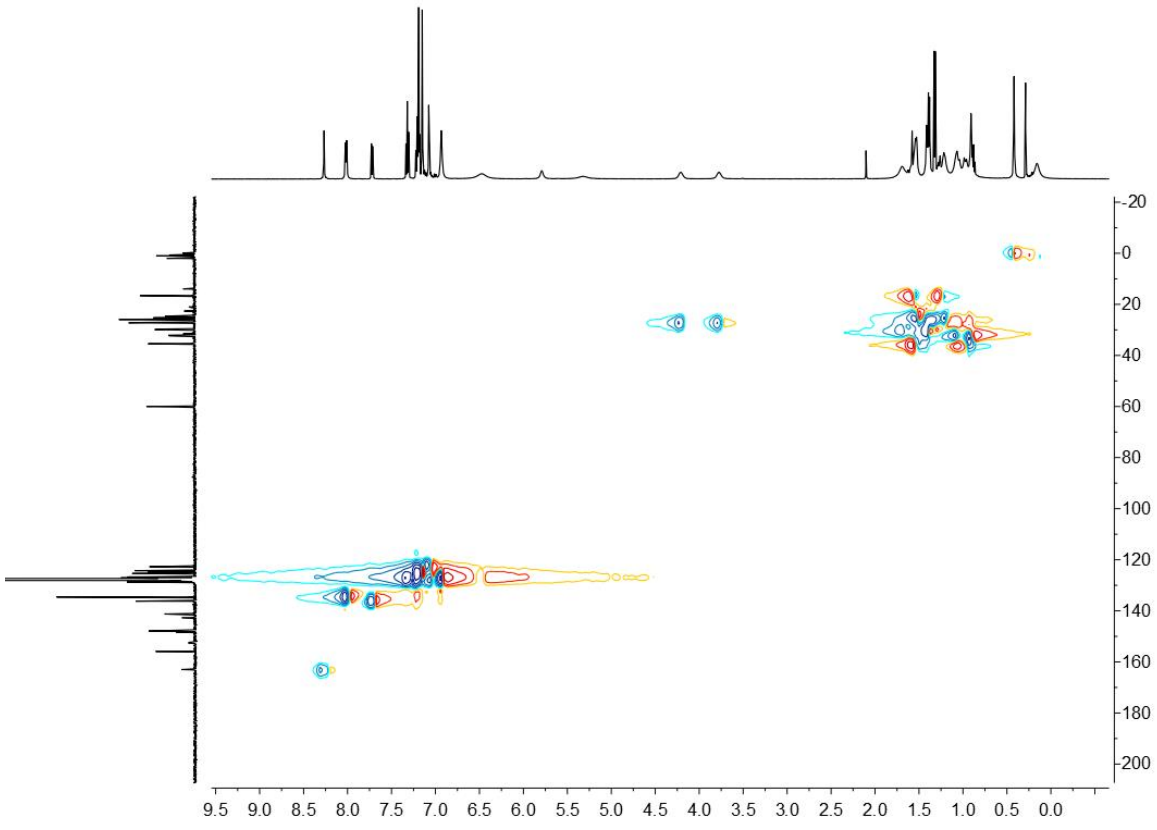

Figure S6-4. ^{1}H,^{13}C-HSQC spectrum of **7** in C_6D_6 at 298 K

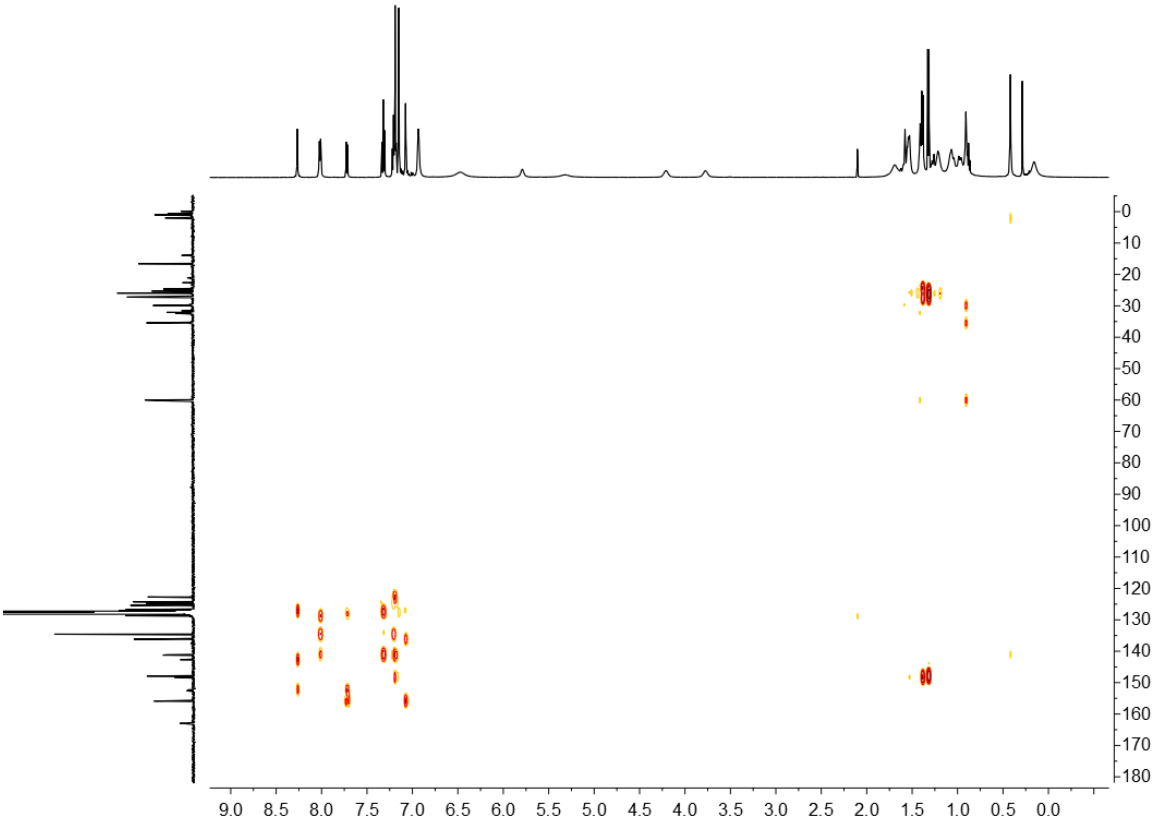

Figure S6-5. $^{1}H,^{13}C$-HMBC spectrum of **7** in C_6D_6 at 298 K

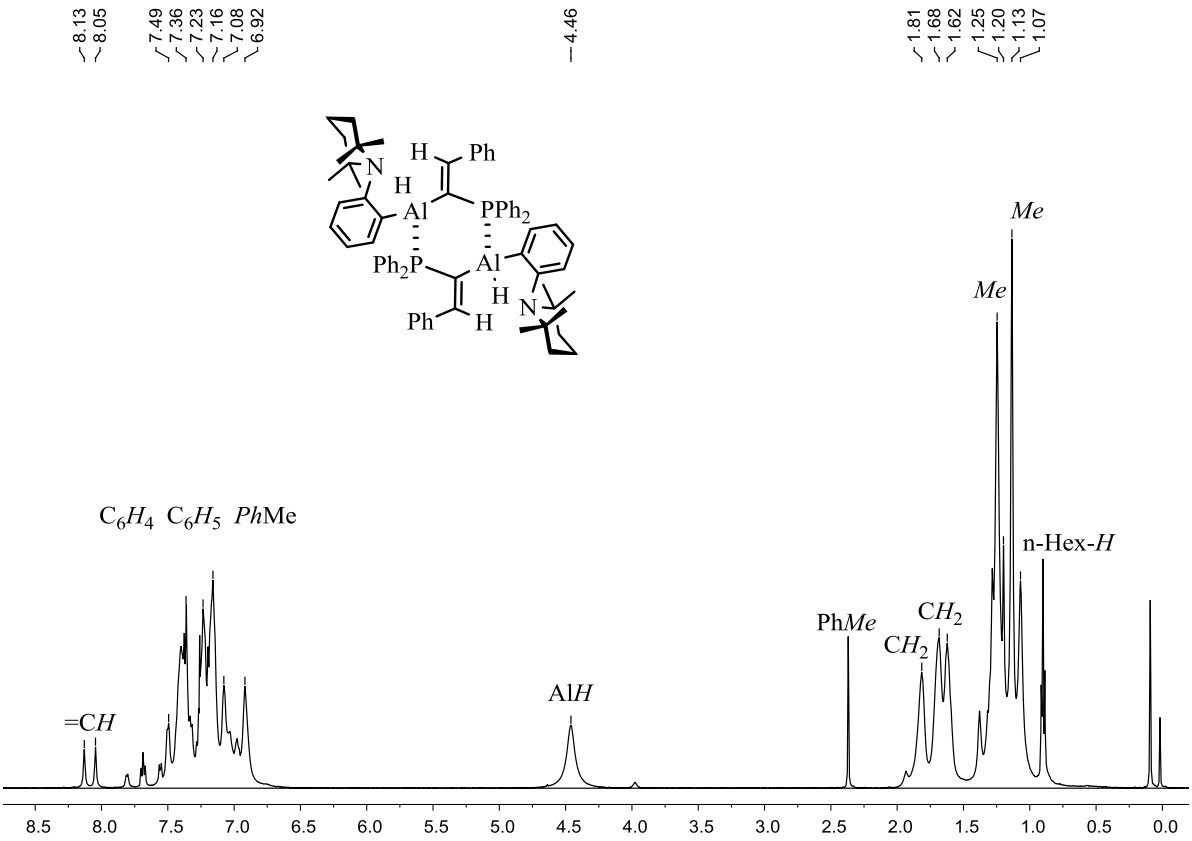

Figure S7-1. ^{1}H NMR spectrum of **8** in $CDCl_3$ at 298 K

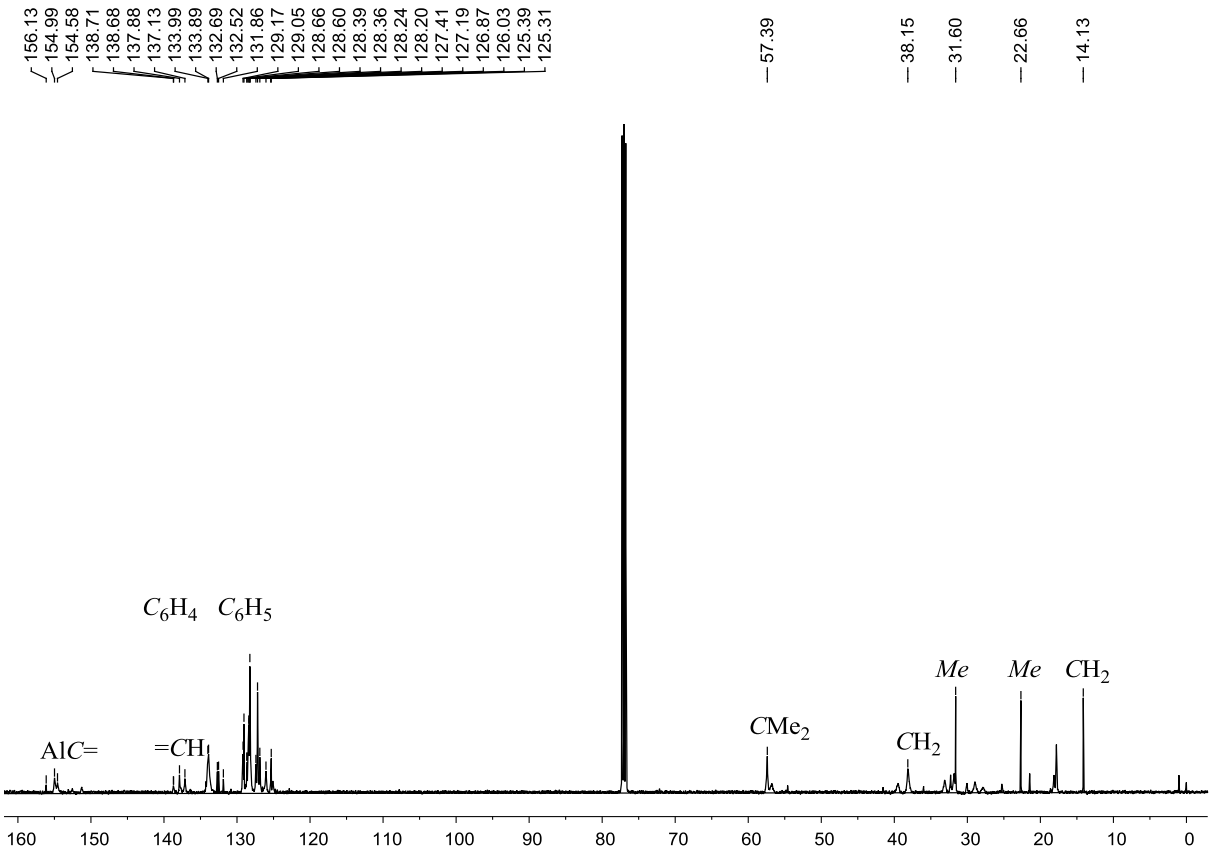

Figure S7-2. ^{13}C NMR spectrum of **8** in $CDCl_3$ at 298 K

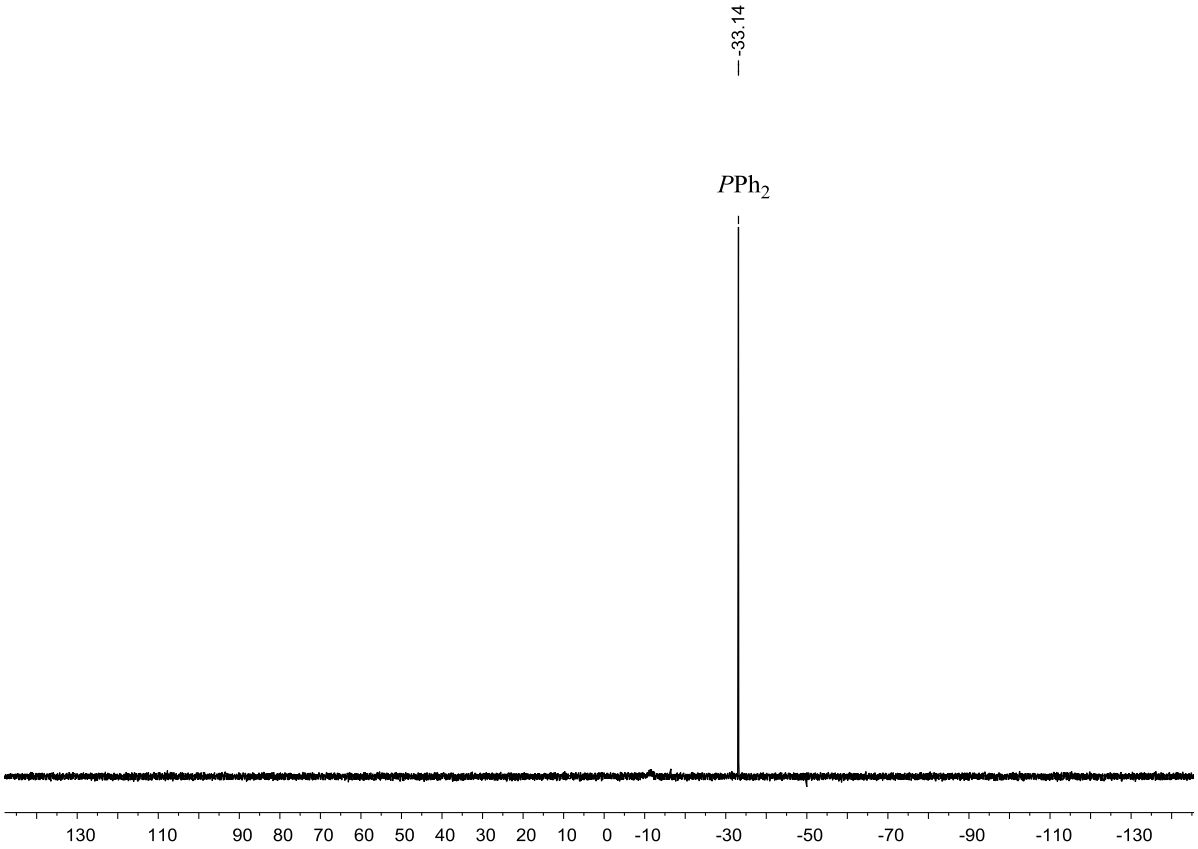

Figure S7-3. ^{31}P NMR spectrum of **8** in $CDCl_3$ at 298 K

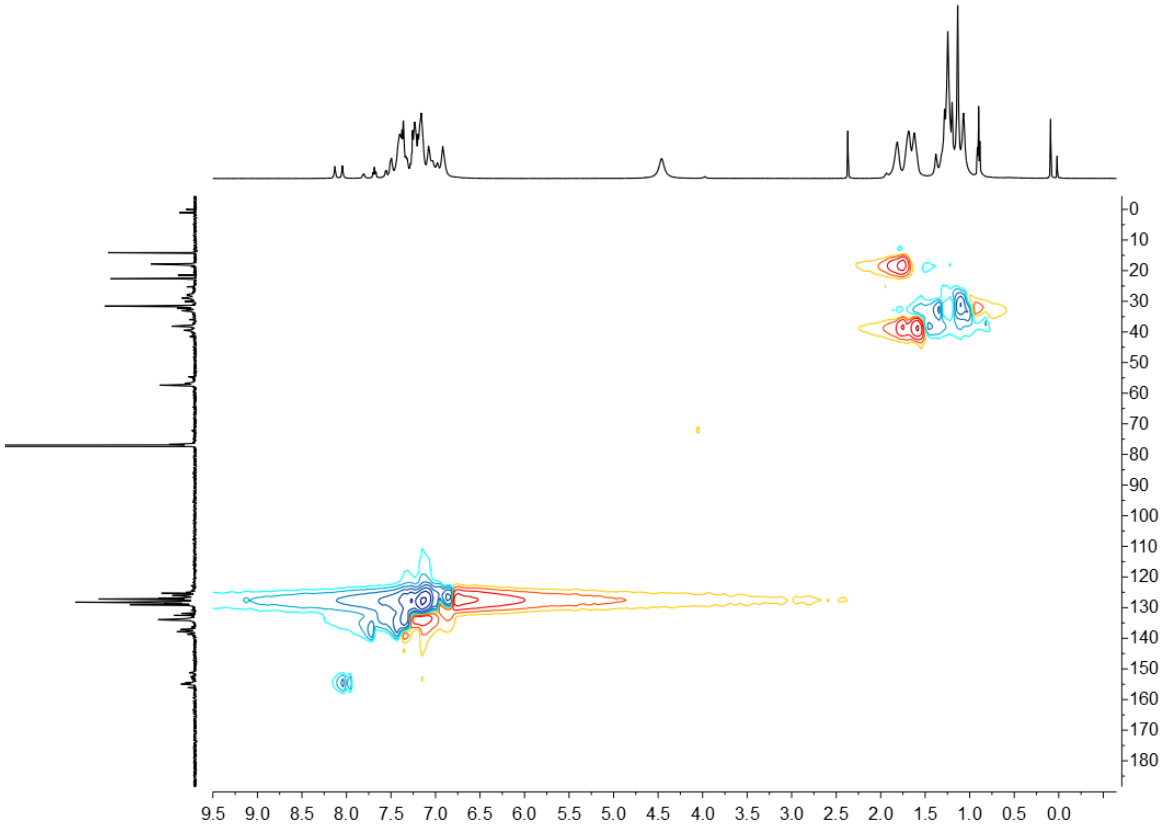

Figure S7-4. $^{1}H,^{13}C$-HSQC spectrum of **8** in $CDCl_3$ at 298 K

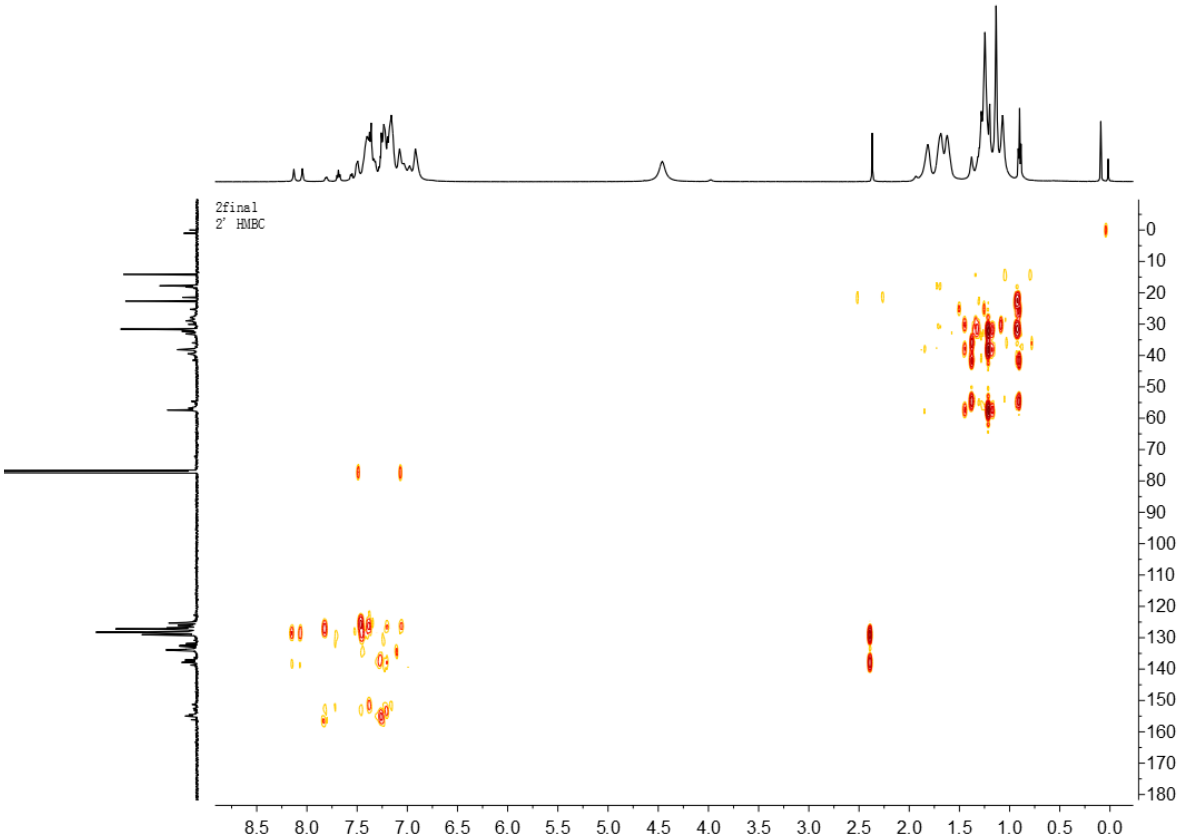

Figure S7-5. $^{1}H,^{13}C$-HMBC spectrum of **8** in $CDCl_3$ at 298 K

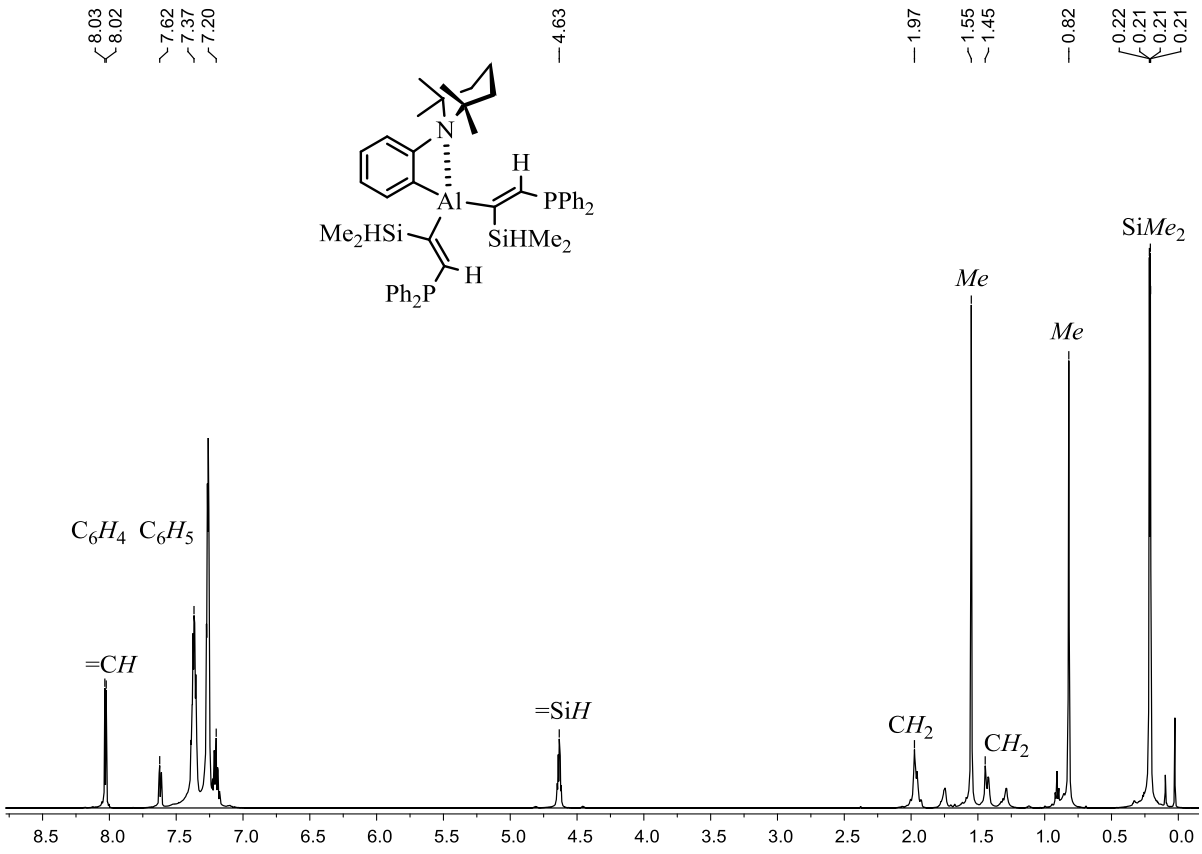

Figure S8-1. ^{1}H NMR spectrum of **9** in $CDCl_3$ at 298 K

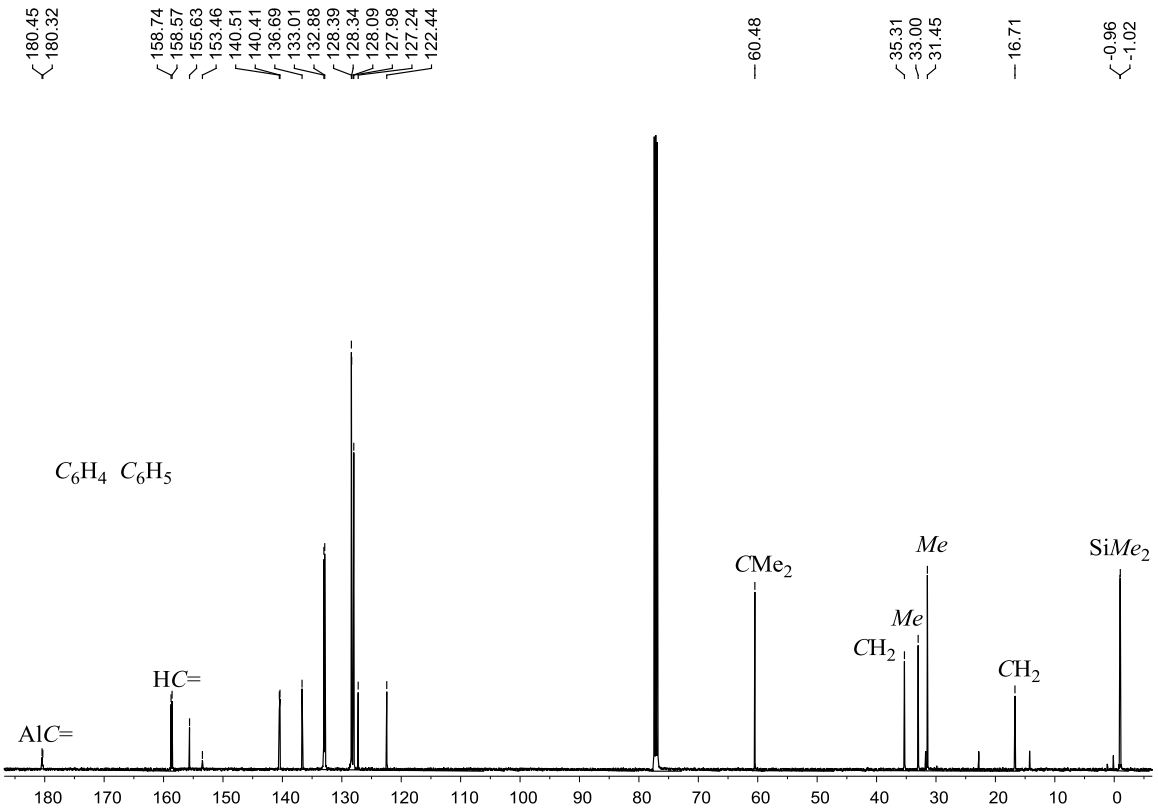

Figure S8-2. ^{13}C NMR spectrum of **9** in $CDCl_3$ at 298 K

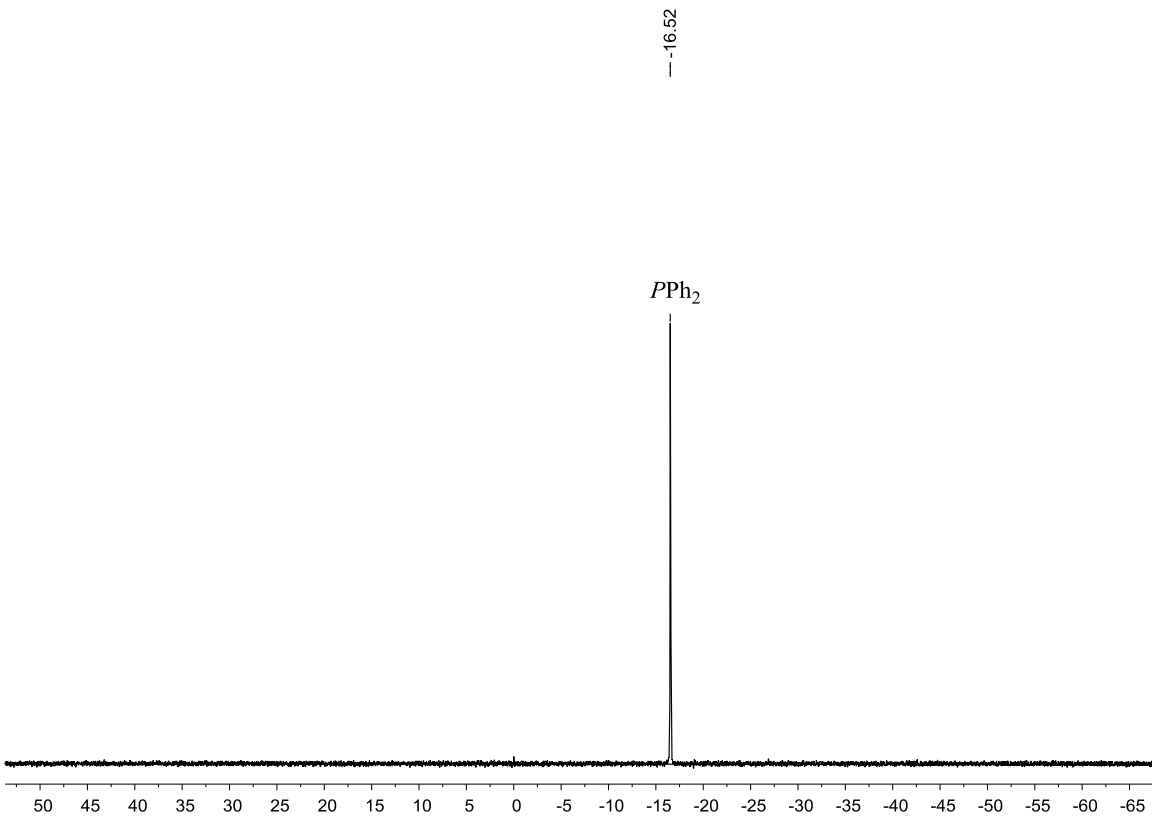

Figure S8-3. ^{31}P NMR spectrum of **9** in $CDCl_3$ at 298 K

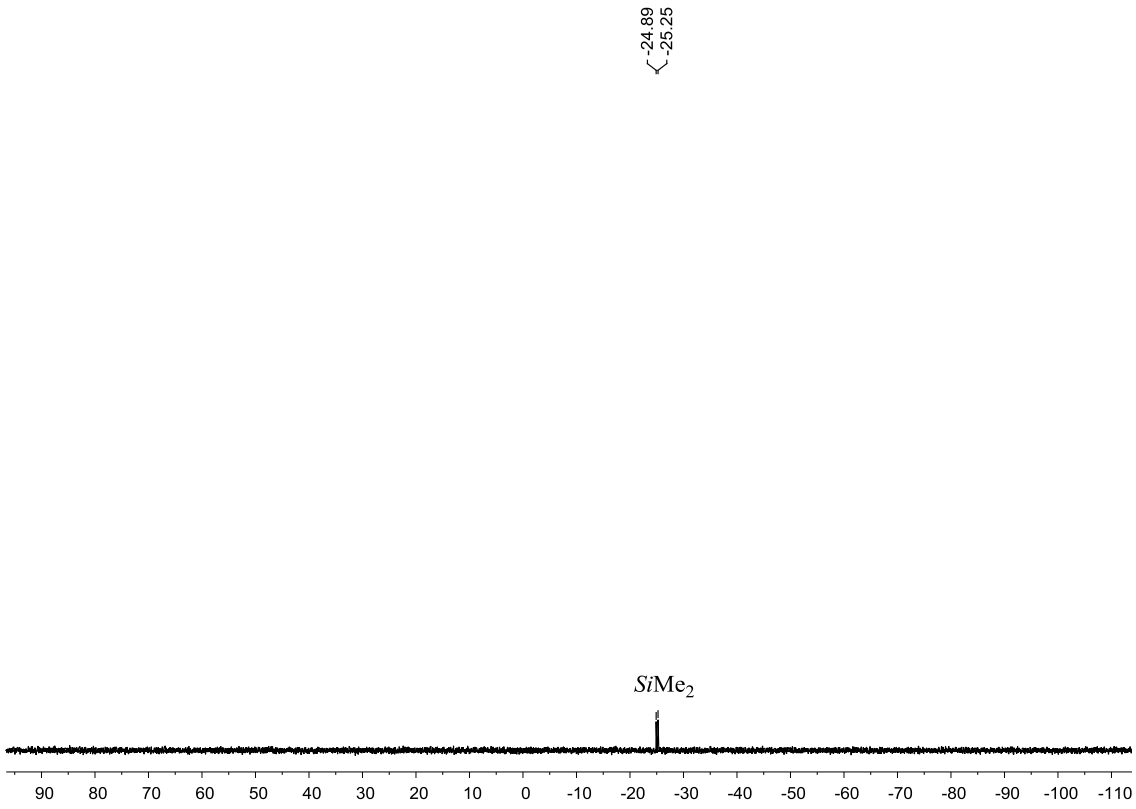

Figure S8-4. ^{29}Si NMR spectrum of **9** in C_6D_6 at 298 K

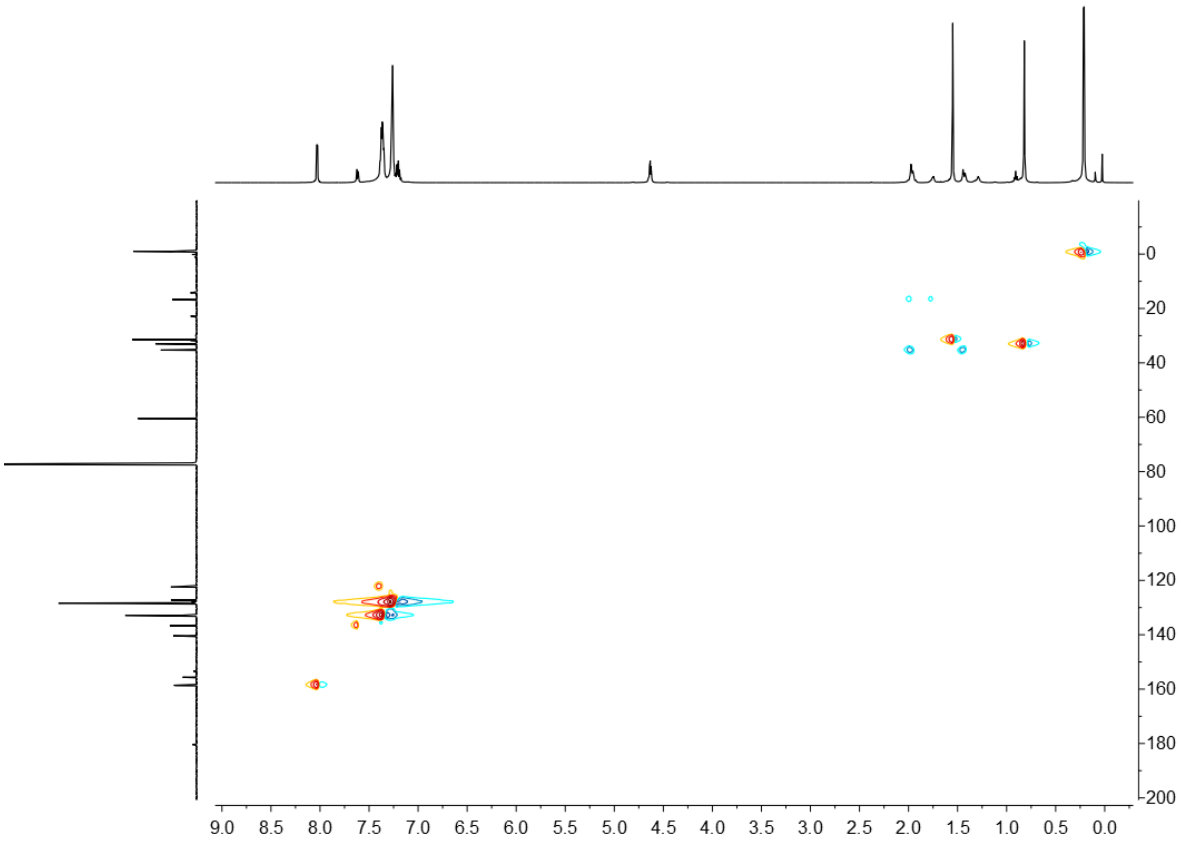

Figure S8-5. $^{1}H,^{13}C$-HSQC spectrum of **9** in $CDCl_3$ at 298 K

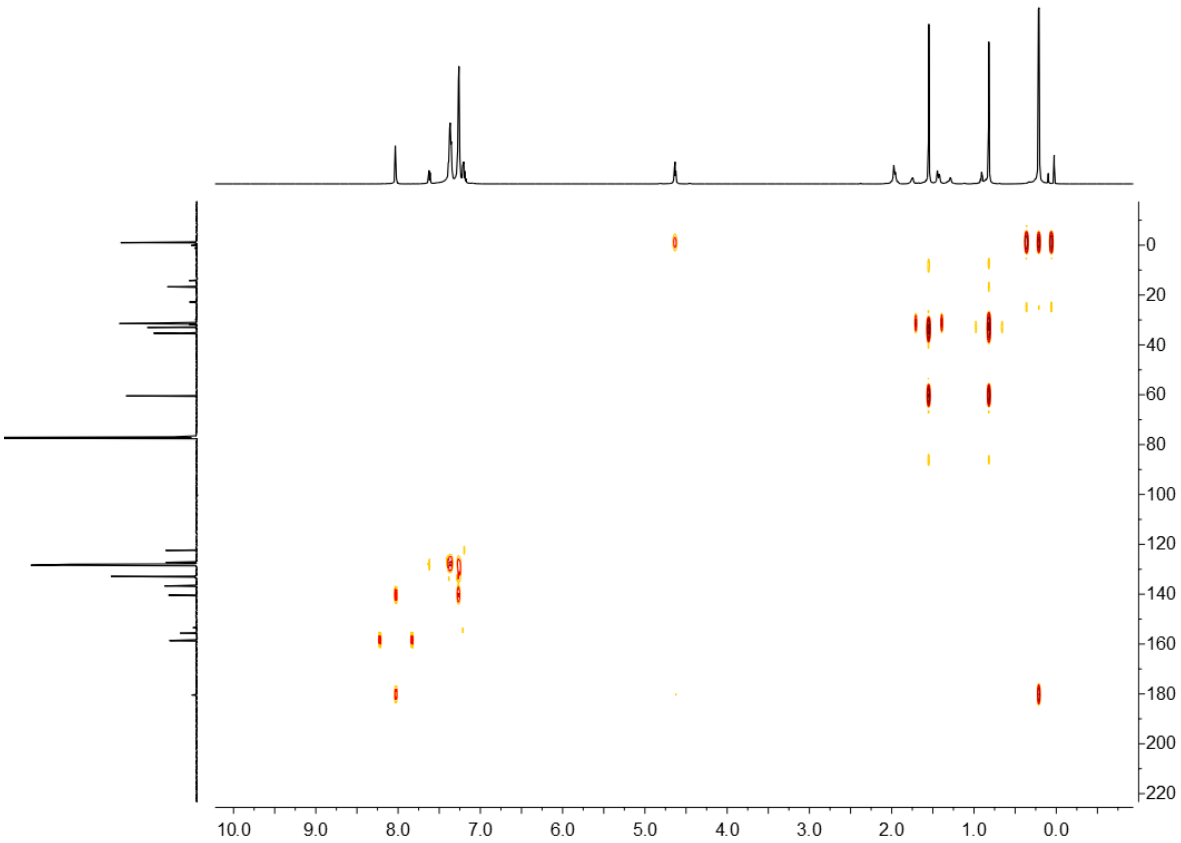

Figure S8-6. $^{1}H,^{13}C$-HMBC spectrum of **9** in $CDCl_3$ at 298 K

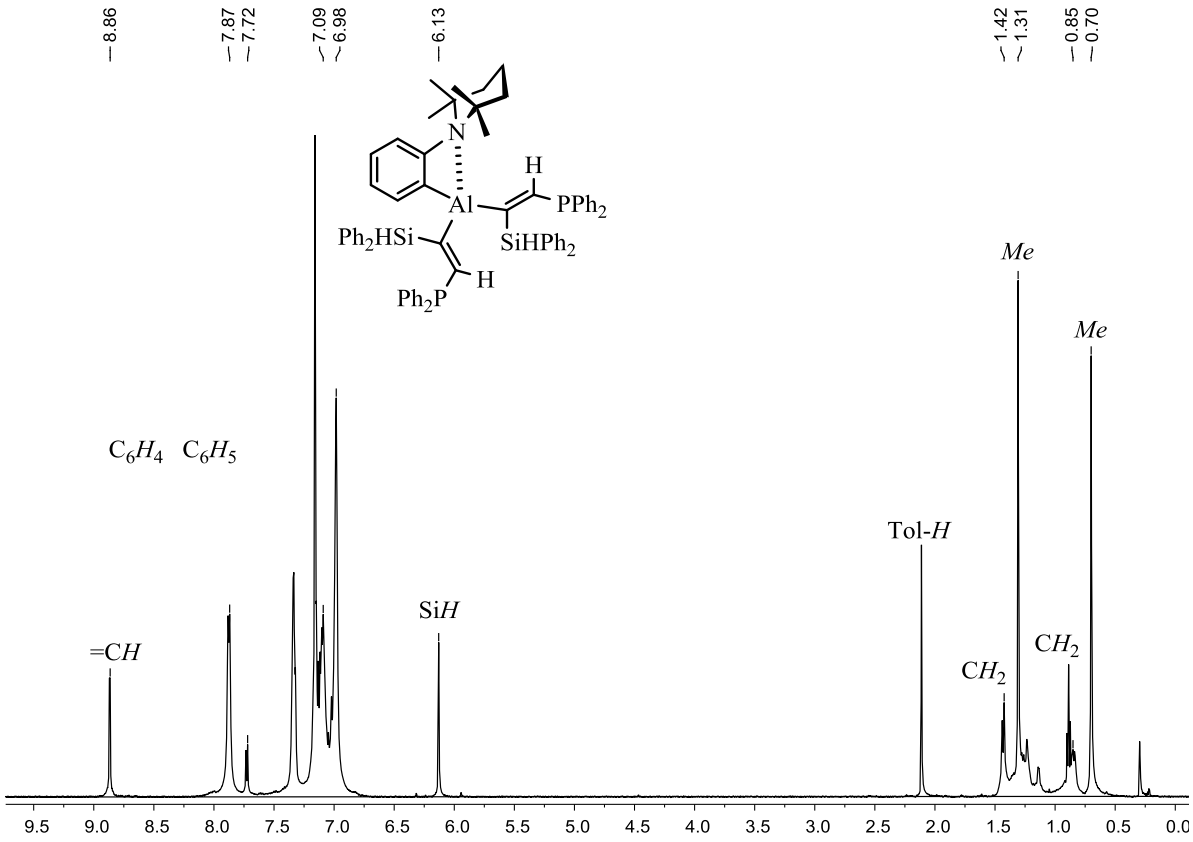

Figure S9-1. ^{1}H NMR spectrum of **10** in C_6D_6 at 298 K

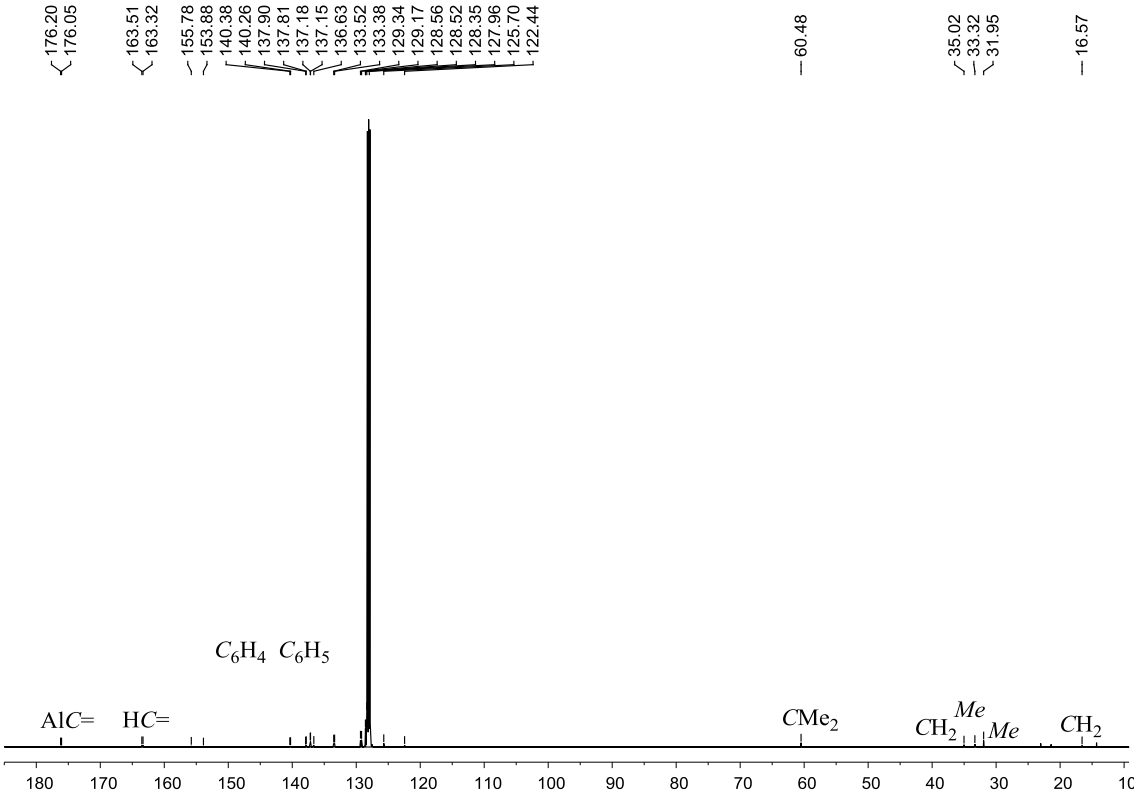

Figure S9-2. ^{13}C NMR spectrum of **10** in C_6D_6 at 298 K

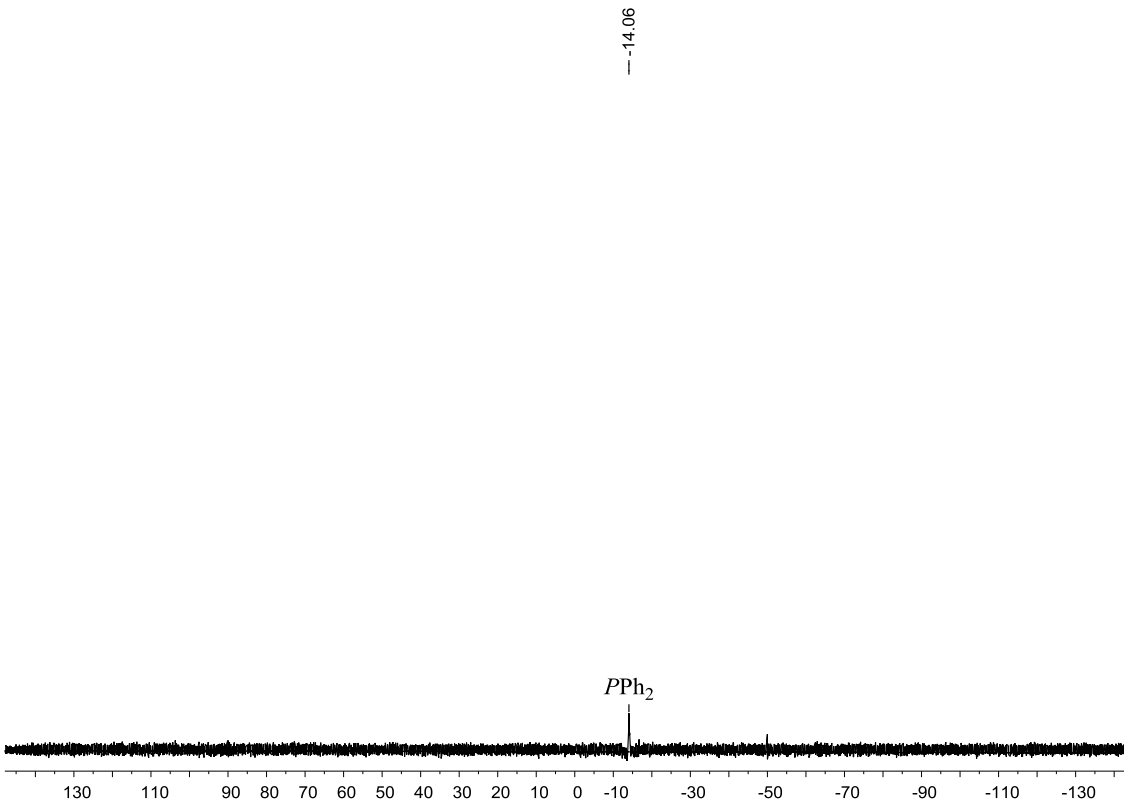

Figure S9-3. ^{31}P NMR spectrum of **10** in C_6D_6 at 298 K

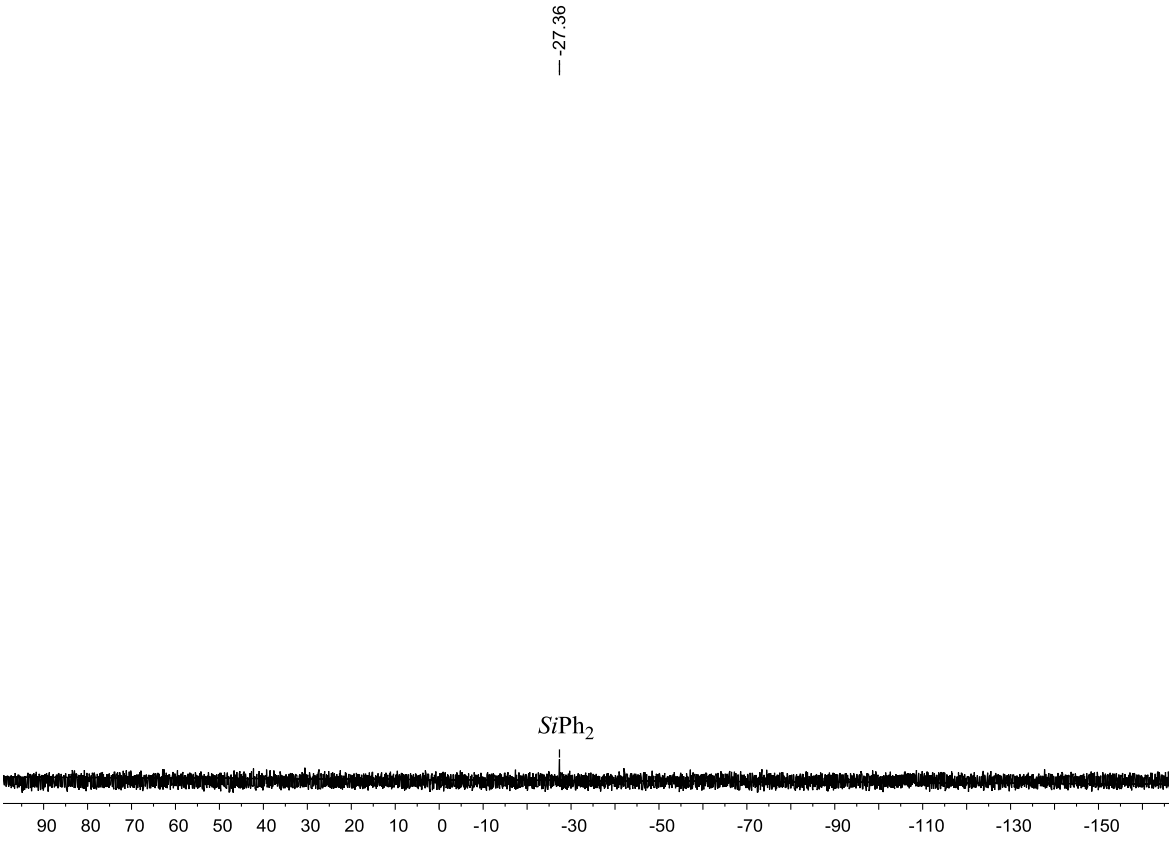

Figure S9-4. ^{29}Si NMR spectrum of **10** in C_6D_6 at 298 K

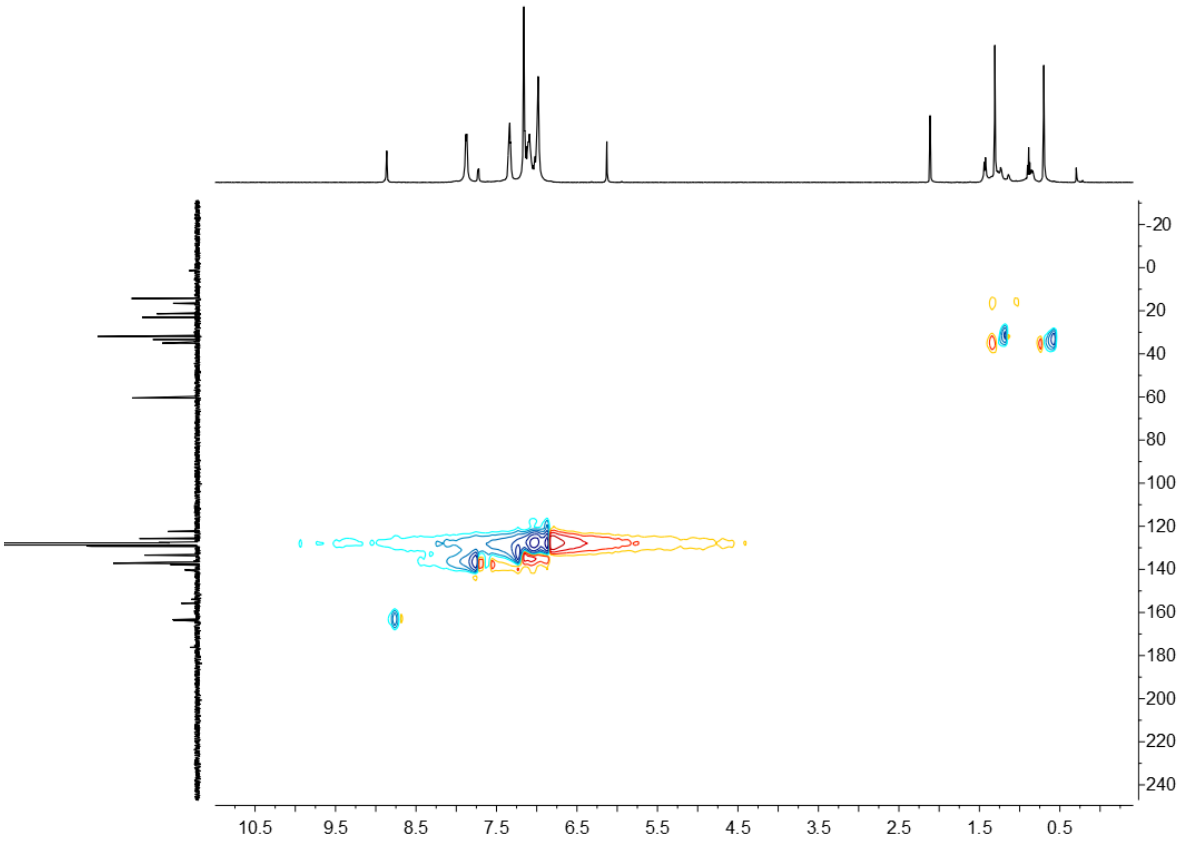

Figure S9-5. $^{1}H,^{13}C$-HSQC spectrum of **10** in C_6D_6 at 298 K

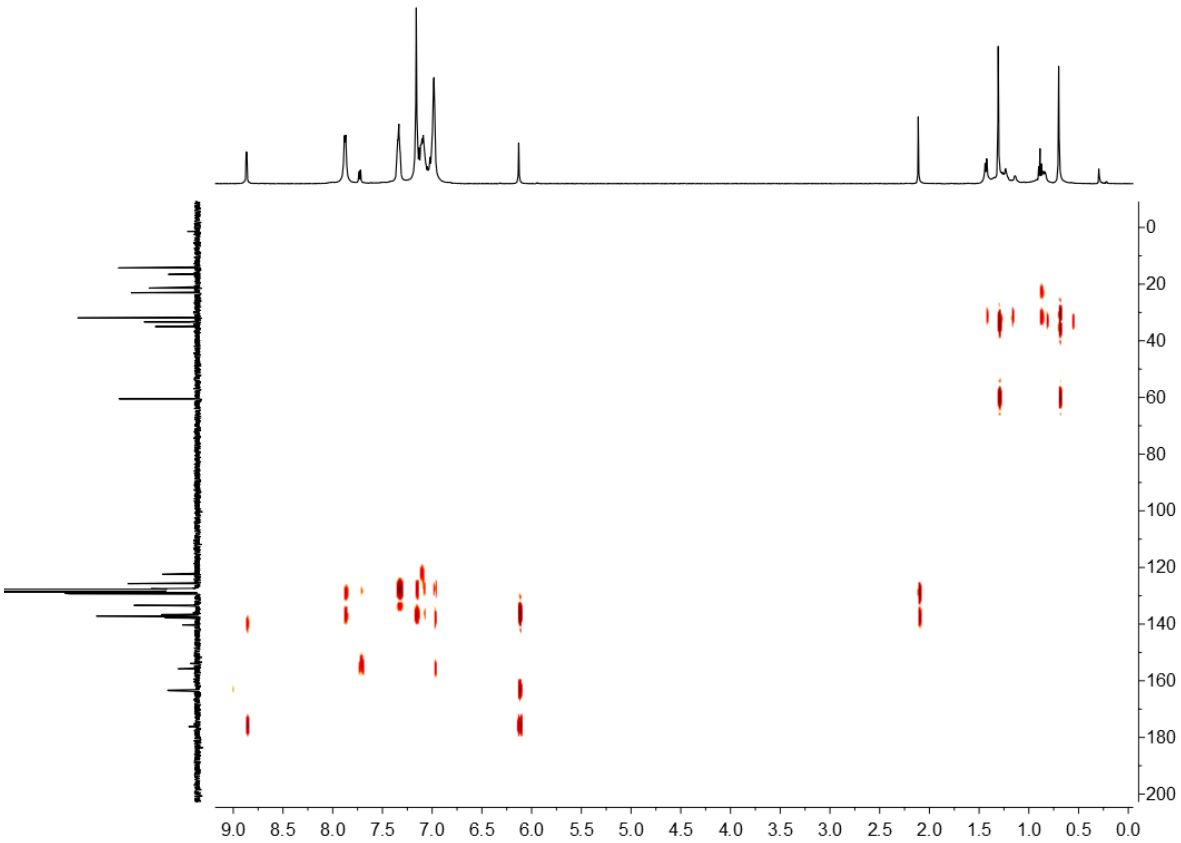

Figure S9-6. $^{1}H,^{13}C$-HMBC spectrum of **10** in C_6D_6 at 298 K

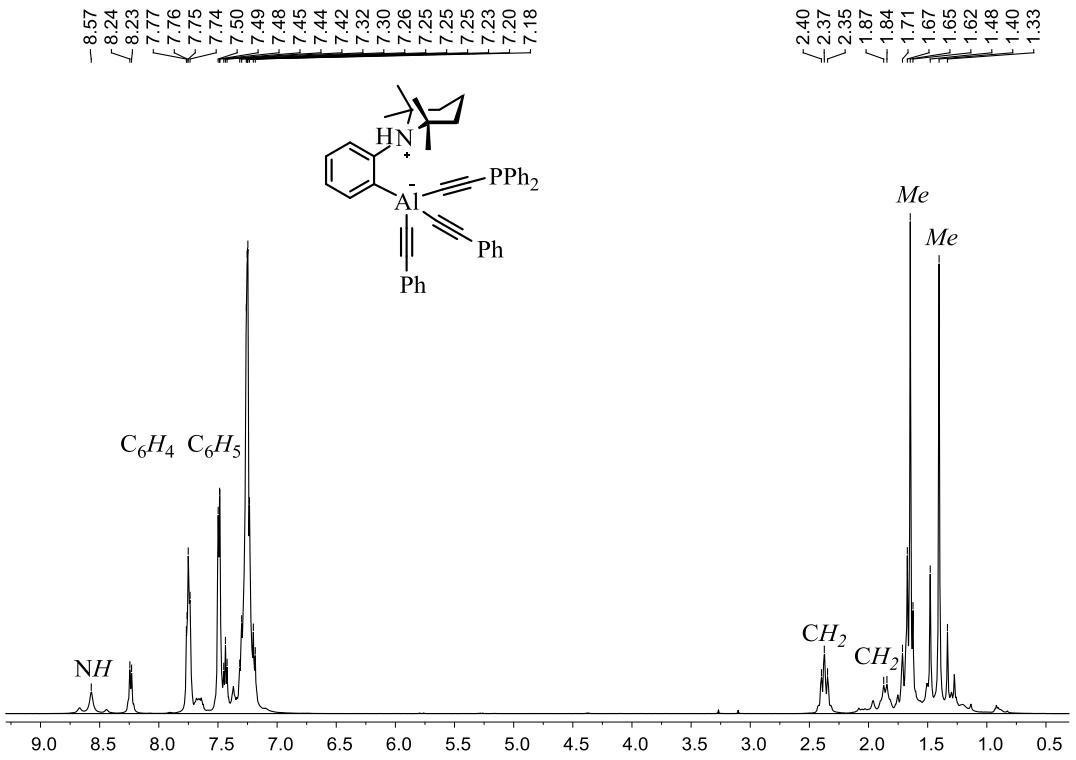

Figure S10-1. ^{1}H NMR spectrum recorded reaction of **2** and one equiv of HC≡CPPh$_2$ to compound [*o*-(TMP)H-C$_6$H$_4$]Al(C≡CPh)$_2$(C≡CPPh$_2$) in C$_6$D$_6$ at 298 K

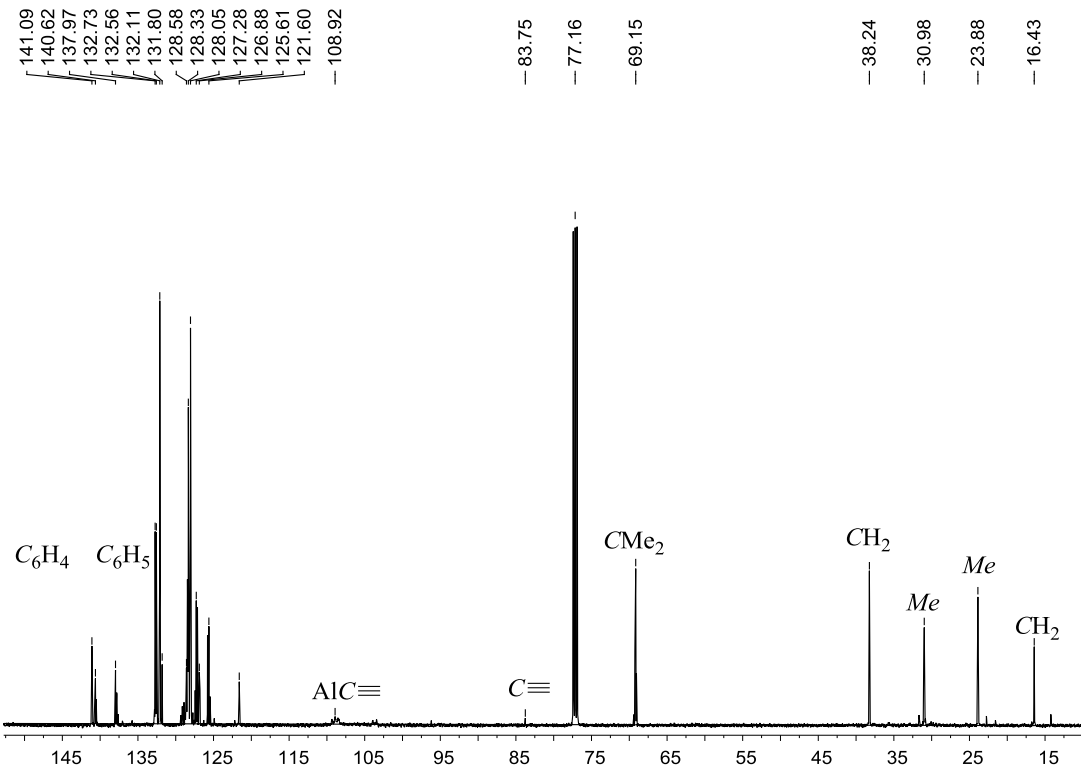

Figure S10-2. ^{13}C NMR spectrum recorded reaction of **2** and one equiv of HC≡CPPh$_2$ to compound [*o*-(TMP)H-C$_6$H$_4$]Al(C≡CPh)$_2$(C≡CPPh$_2$) in C$_6$D$_6$ at 298 K

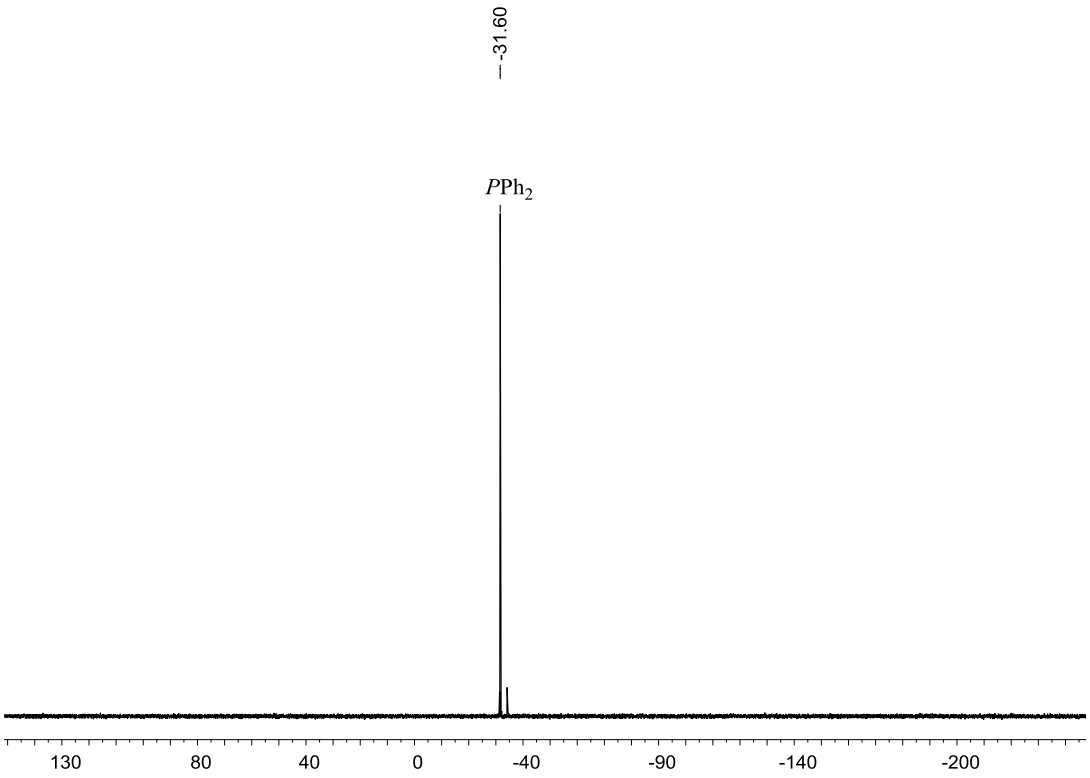

Figure S10-3. ^{31}P NMR spectrum recorded reaction of **2** and one equiv of HC≡CPPh$_2$ to compound [*o*-(TMP)H-C$_6$H$_4$]Al(C≡CPh)$_2$(C≡CPPh$_2$) in C$_6$D$_6$ at 298 K

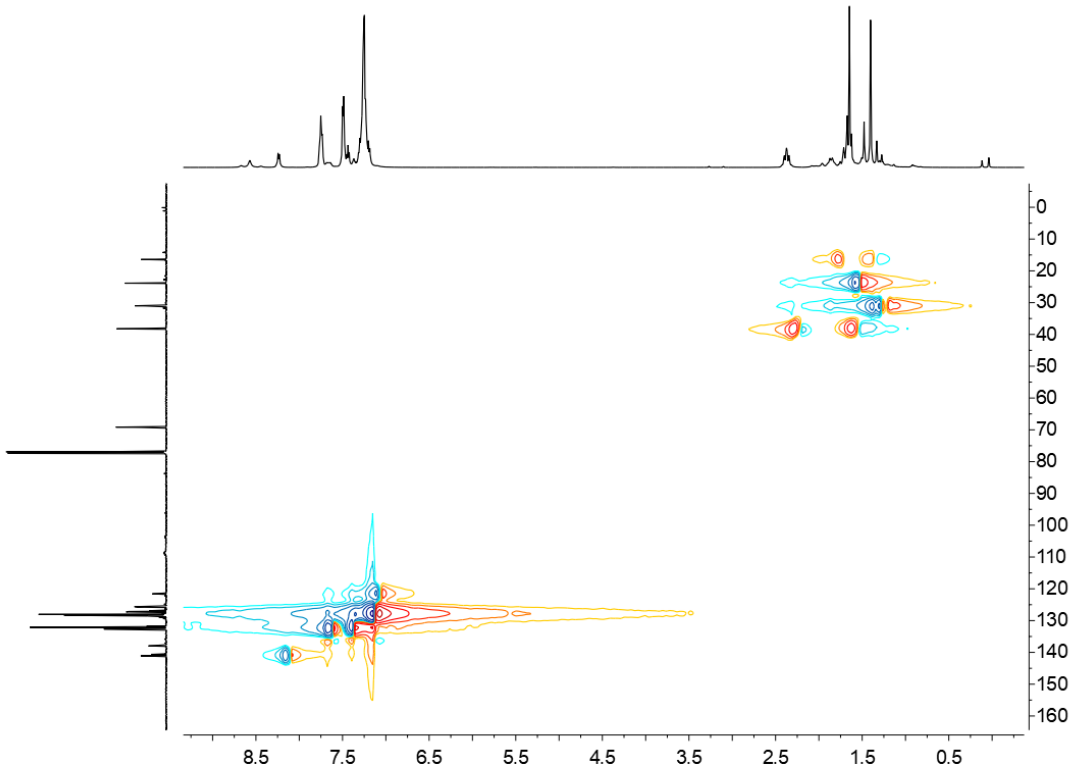

Figure S10-4. ^{1}H,^{13}C-HSQC spectrum recorded reaction of **2** and one equiv of HC≡CPPh$_2$ to compound [*o*-(TMP)H-C$_6$H$_4$]Al(C≡CPh)$_2$(C≡CPPh$_2$) in C$_6$D$_6$ at 298 K

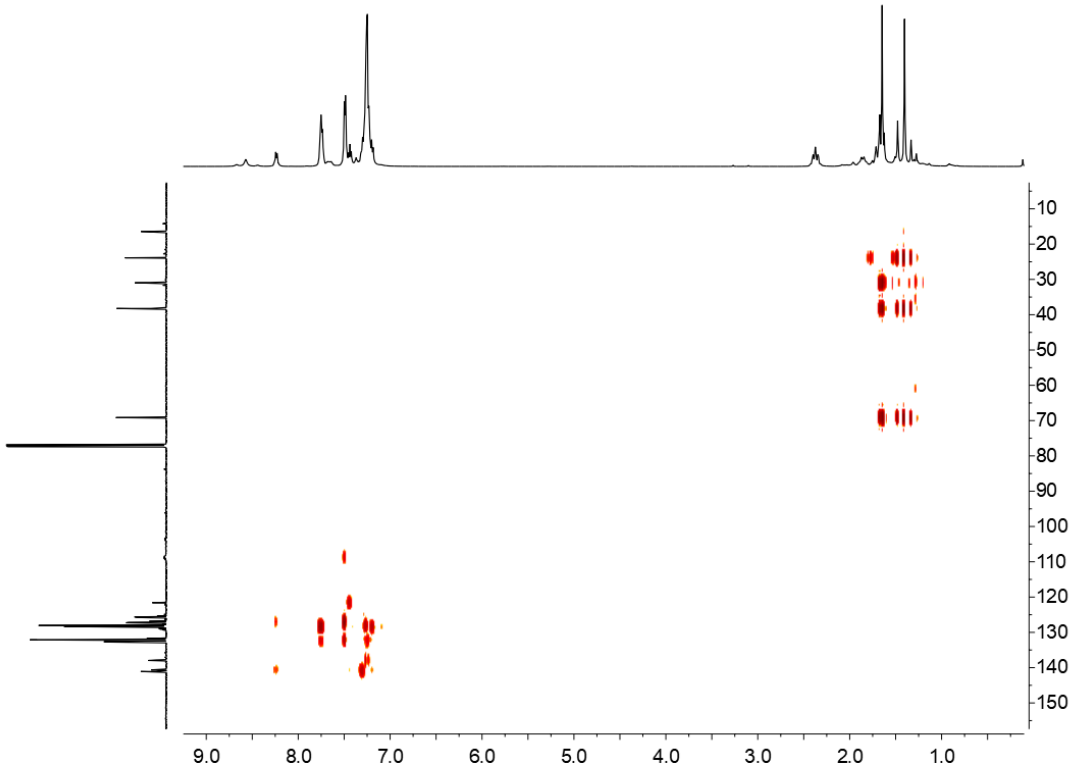

Figure S10-5. $^{1}H,^{13}C$-HMBC spectrum recorded reaction of **2** and one equiv of $HC{\equiv}CPPh_2$ to compound [*o*-(TMP)H-C_6H_4]Al($C{\equiv}CPh)_2(C{\equiv}CPPh_2$) in C_6D_6 at 298 K